

---

Wayne State University Dissertations

---

January 2019

## Molecular Mechanisms In Cftr-F508del Degradation And The Functional Defect Of Cftr Absence In Rabbits

Carthic Rajagopalan

Wayne State University, [crajagop@med.wayne.edu](mailto:crajagop@med.wayne.edu)

Follow this and additional works at: [https://digitalcommons.wayne.edu/oa\\_dissertations](https://digitalcommons.wayne.edu/oa_dissertations)

 Part of the [Physiology Commons](#)

---

### Recommended Citation

Rajagopalan, Carthic, "Molecular Mechanisms In Cftr-F508del Degradation And The Functional Defect Of Cftr Absence In Rabbits" (2019). *Wayne State University Dissertations*. 2290.  
[https://digitalcommons.wayne.edu/oa\\_dissertations/2290](https://digitalcommons.wayne.edu/oa_dissertations/2290)

This Open Access Dissertation is brought to you for free and open access by DigitalCommons@WayneState. It has been accepted for inclusion in Wayne State University Dissertations by an authorized administrator of DigitalCommons@WayneState.

**MOLECULAR MECHANISMS IN CFTR-F508DEL DEGRADATION AND THE  
FUNCTIONAL DEFECT OF CFTR ABSENCE IN RABBITS**

by

**CARTHIC RAJAGOPALAN**

**DISSERTATION**

Submitted to the Graduate School

of Wayne State University,

Detroit, Michigan

in partial fulfillment of the requirements

for the degree of

**DOCTOR OF PHILOSOPHY**

2019

MAJOR: PHYSIOLOGY

Approved By:

---

Advisor

Date

---

---

---

---

---

**© COPYRIGHT BY  
CARTHIC RAJAGOPALAN  
2019  
All Rights Reserved**

## **DEDICATION**

I would like to dedicate this work to my parents, Rajaratnam and Latha Rajagopalan who I consider as the most influential people in my life. From an early age they instilled in me hard work and dedication in anything that I intended to do. They taught me about sacrifice and how to live a life of passion and integrity.

This work is also dedicated to my baby sister, Thiviya Rajagopalan. Thiviya is one of the strongest people I know, who has always looked out for me, especially since I've come to Detroit. She has always inspired me through her strength. This work could not have been accomplished without the sacrifices and patience my sister had to endure.

Finally, this work is also dedicated to my baby brother, Sanchai Rajagopalan. He has always supported me through everything I've done and always has pushed me to be a better person. His determination and mental fortitude have inspired me to continue to strive for greatness.

## ACKNOWLEDGEMENTS

I would like to acknowledge my advisor Dr. Fei Sun for his tremendous support and in bringing this work to fruition. His strength and determination will always be a source of inspiration for me. I remember when I first met with him when was trying to rotate in laboratory. His enthusiasm and drive sold me on that very first meeting. I am grateful for constructive criticism and his daily motivation. His leadership has pushed me to become the scientist that I am today, and he provided me with life tools that I will use for the rest of my life.

I would also like to acknowledge my co-mentor, Dr. Xuequn Chen. Dr. Chen provided me with much needed support and guidance throughout my career as a graduate student. I would also like to thank him for pushing me to become a well-rounded scientist who can stand on his own two feet.

I would also like to thank all my members of my dissertation committee: Drs. J.P. Jin, Bhanu Jena, Youming Xie, and Kezhong Zhang. One could not ask for a more committed and intelligent group people to guide my doctoral project.

I also thank the members of the lab: Dr. Xia Hou, Dr. Honguang Wei, Dr. Mohamed Bouhamdan, and Mr. Brandon Laethem. You have all provided much needed strength and support throughout my graduate career. You guys make coming into the lab a happy, fun experience, and I will always be thankful for that.

I would also like to thank Dr. Jie Xu and his laboratory for helping in the developing the rabbit CFTR Knockout model. Without their help, this project could not have been accomplished.

I thank Ms. Christine Cupps, for I would not be in the position that I am in without her. I thank her for her support and guiding me throughout my career. She has always been of source of strength for me, especially during times of hardship. The Greatest.

Finally, I would like acknowledge Dr. Christos Strubakos, Dr. Akshata Naik, Brent

Formosa, James Woods, Dr. Ken Lewis, and Dr. Josh Holcomb for their support throughout my graduate career.

## TABLE OF CONTENTS

Dedication.....	ii
Acknowledgments.....	iii
List of Tables.....	vii
List of Figures.....	viii
List of Abbreviations.....	ix
Chapter 1: Introduction.....	1
Cystic Fibrosis.....	1
CFTR.....	1
CFTR Protein Structure.....	3
CF Classifications.....	4
CFTR and Endoplasmic Reticulum Associated Degradation (ERAD).....	6
Ubiquitin Proteasome System (UPS).....	8
Conclusions.....	11
Chapter 2: Introduction of Cystic Fibrosis Animal Models.....	11
CF Animal Models.....	11
Conclusions.....	14
Specific Aims.....	14
Chapter 3: Degradation of CFTR-F508del By the E3 Ligase RNF19B and the Ubiquitin E2 Conjugating Enzyme UBE 2L6.....	16
Introduction.....	16
Methods.....	18
Results.....	22
Discussion.....	32
Chapter 4: Functional Defect of CFTR absence in Rabbits.....	36
Introduction.....	36

Methods.....	37
Results.....	43
Discussion.....	51
Conclusions and Future Directions.....	53
Appendix IACUC Approval Letter.....	55
References.....	56
Abstract.....	77
Autobiographical Statement.....	79

## LIST OF TABLES

Table 1: CFTR Related Characteristics Among Species.....	14
--	----

## LIST OF FIGURES

Figure 1. E3 ubiquitin ligase siRNA Library Screen.....	23
Figure 2. RNF19B ubiquitinates F508del and colocalizes with F508del in the ER.....	24
Figure 3. RNF19B over-expression accelerates F508del-CFTR degradation.....	25
Figure 4. Silence of RNF19B increased F508del Expression and RNF19B mediates F508del degradation in a dose-dependent manner.....	26
Figure 5. Silence of RNF19B promotes VX-809-mediated F508del trafficking to the plasma membrane and enhances F508del-CFTR function.....	27
Figure 6. UBE 2L6 over-expression increase F508del degradation.....	29
Figure 7. Silencing UBE 2L6 in F508del-CFBE cells decrease F508del degradation.....	30
Figure 8. UBE 2L6 knockdown enhances F508del function.....	31
Figure 9. Characterization of CF respiratory tract expression and function.....	44
Figure 10. Malformation of tracheal cartilaginous rings in CF rabbits.....	47
Figure 11. Mucus accumulation and inflammation in the lower airways of CF vs WT rabbits.....	48
Figure 12. Characterization of bacteria in bronchoalveolar lavage (BAL) from CF vs. WT rabbits.....	49
Figure 13. Characterization of bacterial infection in bronchoalveolar lavage (BAL) from a moribund CF rabbit and WT age-matched control.....	50

## LIST OF ABBREVIATIONS

ABC: ATP-binding Cassette

BAL: Bronchoalveolar lavage

BALF: Bronchioalveolar lavage fluid

CACC: calcium-activated Cl<sup>-</sup> channel

CHX: cycloheximide-chase

CF: cystic fibrosis

CFBE: cystic fibrosis bronchial epithelial cells

CFTR: cystic fibrosis transmembrane conductance regulator

CFTR-F508del: F508del

COPD: Chronic obstructive pulmonary disease

ECL: Extracellular loop

ER: endoplasmic reticulum

FSK: Forskolin

IB: immunoblot

IBMX: isobutylmethylxanthine

IP: immunoprecipitation

ICL: Intracellular loop

I<sub>sc</sub>: Short-circuit current

MI: Meconium Ileus

NBD: Nuclear Binding Domain

PKA: Protein Kinase A

PKC: Protein Kinase C

PM: plasma membrane

PTC: Premature termination codon

R-Domain: Regulatory Domain

RNF: Ring Finger protein

siRNA: small interfering RNA

SMG: Submucosal Gland

TMD: Membrane spanning domain

UBE: ubiquitin-conjugating enzyme

UPS: ubiquitin-proteasome system

WBC: White blood cells

Wild-type CFTR: WT-CFTR

VCP: Valosin-containing protein

VIMP: VCP-interacting protein

## CHAPTER 1: INTRODUCTION

### Cystic Fibrosis

Cystic fibrosis (CF) is the most common, fatal autosomal recessive disease, with a disease frequency of 1 in 2000 live births and a carrier rate of approximately 5% in the Caucasian population [1]. CF can be characterized as a failure of exocrine tissue in which there is an aberration in the regulation of epithelial Cl<sup>-</sup> channel which is associated with pathophysiology of the disease [2]. The major clinical signs and symptoms of CF include chronic pulmonary disease, pancreatic exocrine insufficiency, intestinal disease, and an increased sweat chloride concentration. With the many major developments in the treatment of CF patients, most of the morbidity and mortality is due to lung disease. The lungs of CF patients become colonized with bacteria which leads to repeated pulmonary infections. The repeated pulmonary infections lead to chronic airway and systemic inflammation, submucosal gland hypertrophy, excessive mucus secretion, impaired mucociliary clearance, and plugging of the small airways that cause progressive bronchiectasis, which eventually leads to lung failure [3-5].

### CFTR

CF is caused by mutations in the cystic fibrosis transmembrane conductance regulator (CFTR), which is a member of the ATP-binding cassette (ABC) transporter superfamily. CFTR is a cAMP-regulated chloride channel found at the apical membranes of most epithelial cells lining the airway and other organs [6]. There are more than 2000 identified CFTR mutations in the CFTR gene (<http://www.genet.sickkids.on.ca/cftr/>). The most common mutation amongst CF patients is the deletion of the phenylalanine residue at position 508 (CFTR-F508del) [7], which is located in the nucleotide binding domain 1 (NBD1). More than 90% of CF patients have at least one copy of the CFTR-F508del (F508del) allele. F508del is unable to achieve a native, folded state that is required for the protein to export from the endoplasmic reticulum (ER) to the apical membrane of

epithelial cells [8], instead the mutant protein is retained in the ER region. There are several lines of evidence that demonstrate the F508del is a folding/processing mutation. Firstly, the F508del mutation is temperature-sensitive, where cells that were incubated at a lower temperature (27°C) lead to the expression of F508del at the plasma membrane [9, 10]. Secondly, cells cultured with high concentrations (>1M) of chemical chaperones, such as glycerol, restores the function of F508del at the plasma membrane [11]. Thirdly, there is assistance of several molecular chaperones on the functional expression of CFTR, whose interactions with F508del is prolonged compared to wild-type (WT) CFTR [12-14]. Fourthly, *in vitro* studies of denaturation and refolding of CFTR fragments corresponding to the first nucleotide binding domain, where F508del is located, have shown that its folding is energetically complex, and the ability of NBD1 with the F508del mutation to reach a native, folded state is impaired compared to the WT NBD1 [15].

When there is a delay in the completion of the native conformation, the CFTR protein is thought to maintain prolonged interaction with molecular chaperones [12-14], which may target the protein for degradation by mechanisms that monitor the ER for misfolded or incompletely complexed proteins. It takes about 10 minutes [16] for CFTR to be created in most cell types, and the assembly of CFTR into a channel is inefficient, where about 99% of newly synthesized F508del is degraded by the ubiquitin proteasome system (UPS), and approximately 60% of the WT-CFTR protein is degraded by the same system [17, 18]. There is substantial evidence demonstrating that misfolded CFTR polypeptides are substrates for the UPS. Firstly, inhibition of the activity of the proteasome by MG-132 cause the accumulation of polyubiquitinated CFTR that can be detected as a characteristic ~7kDa ladder [19, 20]. Second, immunoprecipitated CFTR from cells treated with proteasome inhibitors resulted in a high molecular mass “smear” that is recognized by a ubiquitin antibody [21]. Third, overexpression of the ubiquitin ligase, CHIP, lead to CFTR degradation [22]. Fourth, knockdown of ER membrane anchored E3 ligases, RMA1 and

gp78 using siRNA protect CFTR from degradation [23, 24]. Fifth, Derlin-1/p97-mediated CFTR protein retrotranslocation from the ER to the cytosol for proteasomal degradation delineates an early pathway of CFTR degradation [24-26] CFTR is the first mammalian integral membrane protein to be identified as a substrate for the ubiquitin-proteasome mediated degradation [19, 21], and is used as a model for many diseases of protein conformation, which account for a diverse set of pathologic etiologies such as neurodegenerative diseases [27].

### **CFTR Protein Structure**

The CFTR protein consists of 1480 amino acids that is organized into five functional domains [6, 28]. CFTR has two membrane-spanning domains (TMD1 and TMD2), two nucleotide-binding domains (NBD1 and NBD2), and one regulatory domain (R). TMD1 and TMD2 are comprised of six transmembrane fragments that form the CFTR channel pore. NBD1 and NBD2 interact with ATP to regulate channel activity opening and closing of the TMDs [29, 30]. Channel activity is also controlled by the interactions of the R domain with the N-terminal cytosolic region of TMD1 [6, 31, 32]. NBD1 and NBD2 binds and hydrolyzes ATP, which then causes a conformational change in TMD1 and TMD2, which eventually allows for the transport of Cl<sup>-</sup> across the cell membrane [33]. Mutations in CFTR can occur in any of the five domains, however, many of the mutations occur in NBD1, including the F508del mutation. Where the specific mutation is located on CFTR can affect the formation or function of the CFTR protein. The domains of CFTR and the connecting sequences that have already been shown to be mutated include: the N-terminal [34, 35], intracellular loops (ICL) [36-42], extracellular loops (ECL) [43-45], transmembrane helices 1 through 12 [30, 46-49], and the C-terminal domain. Because the F508del mutation is found on NBD1, this domain has been studied more intensively. The F508del mutation is found in 90% of CF patients, and this mutation on NBD1 causes the destabilization of the CFTR protein [50-52] ATP-binding occurs in both NBD1 and NBD2, which than leads to the

hydrolysis of intracellular ATP to ADP [50, 53]. This leads to conformational changes that allow the CFTR channel to transition from an open to closed state, therefore controlling the gating kinetics of the channel. Other NBD1 mutations, such as G542X and G551D, also have aberration in channel gating [50-52, 54]. The channel activity of CFTR is not only controlled by NBD1 and NBD2, but also with the R domain. The activation of the CFTR channel is dependent on the phosphorylation by cAMP-dependent protein kinase A (PKA) [41, 55]. There are reports that CFTR can be phosphorylated by other protein kinases including protein kinase C (PKC), cyclic GMP activated protein kinase, Src kinase and casein kinase II [55]. Also, there are multiple phosphorylation sites on the R domain which can help modulate specific domain-domain interactions that are stimulated by PKA [41]. Mutations of the R domain, such as D648V, E664X, E656X, and 2108delA, disrupt R domain function, which results in aberrant gating of the CFTR channel [56, 57].

### **CF Classifications**

The more than 2000 different CF mutations can be categorized based on the dysfunctions of CFTR at different levels of maturation and function of the channel. Traditionally, these mutations were grouped by CFTR function (Classes I, III, IV, and VI) or CFTR processing (Classes I,II, and V) [58-60].

#### ***Class I mutations***

Class I mutations include nonsense mutations, splice mutations, or deletions, that introduces a premature termination codon (PTC), that prevent functional CFTR biosynthesis. 22% of CF patients have at least one mutation in this class. G542X, W1282X, and, R553X are examples of Class I mutations.

#### ***Class II mutations***

Class II mutations include a missense mutation which causes the CFTR protein to be

produced, however CFTR is misfolded and is degraded by the ER quality control system, keeping the protein from trafficking to the cell surface. About 90% of CF patients have at least one mutation in this class. F508del, N1303K, and 1507del are examples of this class of mutation.

### ***Class III mutations***

Class III mutations are missense mutations that produces a non-functioning, unstable protein that can traffic to the cell surface. These types of mutations are also called gating mutations and about 6% of people with CF have this mutation. Examples of Class III mutations are G551D and S549N.

### ***Class IV mutations***

Class IV mutations include missense mutations which produces a CFTR channel with less conductance. This conductance is decreased because of an abnormal conformation of the pore, resulting in aberrant ion flow. These mutations account for about 6% of CF patients. Examples of this class of mutations include D1152H, R347P, and R117H.

### ***Class V mutations***

Class V mutations introduce splicing of promotor defects in the CFTR gene, leading to a reduced amount of CFTR protein at the cell surface. These mutations affect gene expression, not the conformational changes of the channel. This class of mutations affects about 5% of individuals with CF. Examples of these types of mutations include 3849+10kbC>T, 2789+5G>A, and A455E.

### ***Class VI mutations***

Class VI mutations increase the turnover of CFTR protein at the cell surface. Even though the CFTR protein is functional, it's highly unstable at the cell surface and is quickly removed from the cell surface and degraded by the lysosome. Example of these types of mutations include rescued F508del, 120del23, N286Y, 4326delITC, and 4279insA.

Even though there are more than 2000 mutations of CFTR, there is a lack of correlation between the genotype and phenotype of CF patients [61]. For example, a study demonstrated that meconium ileus (MI) only developed in a subset of CF patients. The study showed that non-CFTR genes contribute to its susceptibility, and the CFTR genotype affects the occurrence of this complication, where patients with the more severe CFTR variants are at risk for MI. It was hypothesized that the susceptibility to MI was influenced by specific CFTR genotypes and that the prevalence of MI can be used to discriminate among severe CFTR mutations [62]. Also, the pleiotropic defects of a single mutation in the CFTR gene has limited the drug therapy effects of certain mutants which have been categorized as Class I, II, or II/III [60]. These problems led to authors proposing in expanding the classification of the major mechanistic categories [6, 28, 63] which accommodates the complex, combinatorial molecular/cellular phenotypes of CF. The new classification consists of 31 possible classes of mutations, including the original classes and 26 combination of the original classes [60]. To illustrate this new classification system, F508del is now classified as Class II-III-VI, where before it was solely Class II. This classification system was further supported by a study by Vertex Pharmaceutical where they tested 54 missense mutations and found that 24 of them had both processing and gating defects [64]. This new classification system is critical in that it allowed individuals for certain mutations to have a broader reach in the type of therapy that is given. For example, when F508del was classified as only a Class II mutation, it was thought that only corrector drugs, such as VX-809, could be used for individuals with this mutation. However, F508del is now classified as Class II-III-VI, which allowed for a new combinatorial drug therapy called Orkambi, which is a combination of VX-809 (corrector) and VX-770 (potentiator), to be used by individuals with the F508del mutation [65].

### **CFTR and Endoplasmic Reticulum Associated Degradation (ERAD)**

The ER provides mechanisms that facilitate the appropriate folding of newly synthesized

secretory and integral membrane proteins, and eliminates proteins that are unable to achieve their native, folded state [66, 67]. The balance of proper folding and disposal of misfolded proteins is vital for cellular homeostasis. When there is an accumulation of irregular proteins, ER stress is evoked, along with the unfolded protein response, which induces the expression of ERAD components to accelerate protein elimination [68, 69]. ERAD is the process in which protein substrates are polyubiquitinated and travel to the cytosol for protein degradation. ERAD can be divided into four steps: recognition, retrotranslocation, ubiquitination, and degradation. These steps include the recognition and the removal of misfolded proteins from the ER, followed by their cytoplasmic ubiquitination and ubiquitin-dependent proteolysis by the 26S proteasome [70-72].

Protein substrates transiting the ER can be soluble or membrane bound with significant portions in the lumen, membrane, and cytosol. To achieve specificity, ERAD employs different mechanisms to monitor protein misfolding. This can be characterized in yeast, in which distinct E3 complexes define different ERAD pathways [73-75]. Membrane and soluble proteins with luminal lesions are delivered to the ERAD-L pathway in which the Hrd1p/Hrd3p ligases form a complex by binding to Der1p via the linker protein Usa1p. Membrane proteins with misfolded cytoplasmic domains uses the ERAD-C pathway, which are directed to the E3 ligase Doa10p [73]. substrates with misfolded intramembrane domains are subjected to the ERAD-M pathway, which differs from the ERAD-L pathway by being independent of Usa1p and Der1p. All three pathways eventually converge at cdc48/AAA p97 ATPase complex [76].

In mammalian cells, the ERAD pathway is more complex. It is poorly understood how ERAD machinery recognizes misfolded protein in the ER, however, there are three potential mechanisms. First, molecular chaperones play a central role in the recognition of misfolded proteins. Examples are Hdj-2 and Aha-1, which are co-chaperones for Hsp70 and Hsp90, respectively. Hdj-2 recognizes F508del twice as much as WT-CFTR [20], while the knock down

of Aha-1 by RNA interference results in a significant amount of F508del maturation [77]. Also, the result that Aha-1 interacts preferentially with CFTR in the region corresponding to the F508del mutation further supports this mechanism [78]. Second, the ubiquitin ligase, CHIP, targets defective proteins whose cytoplasmic domains are recognized by the cytoplasmic chaperones of the Hsp70-Hsp90 family [12-14]. Third, Derlin-1 mediated CFTR degradation plays a role in recognizing misfolded membrane or transmembrane proteins [24-26].

After the recognition process, misfolded proteins are transported to the cytoplasm for proteasomal degradation, a process which is called dislocation or retrotranslocation [79, 80]. The retrotranslocation machinery consists of p97 (VCP), Derlin-1 and valosin-containing protein (VCP)-interacting membrane protein (VIMP) [81]. Derlin-1 may form a retrotranslocation channel in the ER membrane and it links their recognition of misfolded ER proteins to the ubiquitin-mediated proteasomal degradation in the cytosol [81, 82].

### **Ubiquitin Proteasome System (UPS)**

Retrotranslocated proteins are subsequently ubiquitinated by the E1-E2-E3 ubiquitin cascade system [83]. In mammalian cells, there are two E1 activating enzymes, about 40 E2 conjugating enzymes and about 1000 E3 ubiquitin ligase enzymes have been identified [84]. The corresponding ubiquitin conjugase (E2) and ligase (E3) have been shown to be specific in the three different ERAD pathways discussed above [73, 74]. In this system, activation of the ubiquitin occurs through an ATP-dependent formation of a high energy thioester bond between the active site cysteine of the E1 activating enzyme [85]. The activated ubiquitin follows the cascade and binds to the E2 conjugating enzyme. Finally, the E3 ubiquitin ligase binds to the E2-bound ubiquitin and the protein substrate, in this case the F508del, and promotes the transfer of the ubiquitin to the substrate [86]. This process occurs several times, where additional ubiquitin molecules are conjugated to the first ubiquitin molecule, form a polyubiquitin chain that is

recognized by the 26S proteasome in the cytosol, where degradation of the polyubiquitinated F508del occurs [87, 88]

The substrate is usually ubiquitinated by an isopeptide bond between the carboxyl end of ubiquitin and lysine primary amine of the substrate. When the poly-ubiquitin chain is formed, another ubiquitin forms another isopeptide bond with a lysine residue of the original ubiquitin. Ubiquitin is a highly conserved 76 amino acid polypeptide that contains seven lysine (K) residues (K6, K11, K27, K29, K33, K48, and K63). All seven lysine residues can be conjugated together to form a poly-ubiquitin chain on substrates topologies [89, 90]. Interestingly, the lysine-linked poly-ubiquitin chains that are formed on F508del seem to be through K11, K48, and K63 linkages, where K11 and K48 linkage facilitate degradation of F508del and K63 linkages prevent degradation. These linkages are important because they are believed to be mediated by the E2 conjugating enzymes [90-93]

There are about 1000 E3 ligase enzymes therefore they demonstrate substrate specificity [68, 94]. While the E3 ligases recognize and bind to the protein substrate, the E2 enzymes catalyzes the transfer of ubiquitin to the substrate. Because F508del is retained and poly-ubiquitinated in the ER, there must be ER resident E3 ligases that recognize F508del. Several E3 ligases have been implicated in F508del degradation including RNF5, CHIP, gp78, Hrd1, Nedd4-2, and RNF185 [95-99] However, other E3 ligases seem to be involved in F508del degradation because previous studies have demonstrated a significant amount of F508del being degraded even when some of the above mentioned E3 ligases were silenced. Also, E2 conjugating enzymes may mediate the different K-linkages that progresses F508del for degradation. Therefore, further studies must investigate other ER resident E3 ligases and their interacting E2 conjugating enzymes that may mediate F508 degradation.

**Conclusion**

There are still some missing links in the F508del degradation, and the purpose of this part of the study is to identify early checkpoints in the ubiquitin proteasome system that recognizes F508del early in its biogenesis in the ER. Previous studies have looked at the degradative machinery involved in CFTR degradation. However, the ER-resident E3 ligases are poorly understood in this process, therefore characterizing their role is crucial for understanding the premature degradation of F508del. Our preliminary data indicate that RNF19B is an E3 ligase that is involved in F508del degradation. This E3 ligase has an interacting E2 conjugating enzyme, UBE2L6. This study will determine if these enzymes mediate the degradation of F508del.

## CHAPTER 2: INTRODUCTION OF CYSTIC FIBROSIS ANIMAL MODELS

### CF Animal Models

There have been major progress in understanding CF pathogenesis since the gene was first cloned in 1989 [7], however, many question remain unanswered, including the pathogenesis of the disease in different organ and their reaction to different therapies [28, 100]. Cell model systems have been important in determining underlying mechanisms; however, they are unable to recapitulate pathogenesis of the disease at complex levels of organs. CF animal models have been crucial in the understanding of the disease pathogenesis and the development of therapeutics for the disease [101], however there are many limitations to these models. Some models fail to reproduce major pulmonary phenotypes that are observed in CF patients or they fail to resolve pathophysiological question such as the roles of abnormal airway superficial epithelium vs. submucosal glands (SMGs) in the pathogenesis of CF lung disease [102-107]. Other larger animal models only live for a short amount of time and/or levy high maintenance costs and require special care which in turn limits their use for the evaluation of different therapeutic agents [101, 108].

#### *Mouse model*

The interruption of the CFTR gene generated a knockout (KO) mice model with no production of normal CFTR [109]. These models are unable to detect spontaneous colonization of *Staphylococcus aureus*, *Haemophilus influenza*, or *Pseudomonas aeruginosa*, bacterial species that cause lung infections in human CF patients [110, 111]. This is due to the fact that mice express low levels of non-gastric H<sup>+</sup>/K<sup>+</sup> adenosine triphosphatase ATP12A, which helps with the exchange H<sup>+</sup> and K<sup>+</sup> ions across the membrane. Therefore, this maintains the pH of the airway surface liquid, which seems to act as a defense in the airway against infections [112]. The mice model is unable to further our understanding on how the disease is initiated and the development of infection. Other differences include insufficient size of the airway and the presence of a non-CFTR calcium-

activated Cl-channel (CACC) that is not similar to humans [58, 113, 114].

### ***Rat model***

The mouse model has many dissimilarities to humans, including that fact the SMGs were only located at the proximal trachea. The rat model, on the other hand, had SMGs that spread to the bronchi, which was similar to humans. Therefore, the CFTR KO rat model was developed [104]. The CFTR KO rats showed congenital tracheal defects and decreased airway surface liquid in the distal airways, similar to what is observed in humans [104]. However, this model is unable to spontaneously develop lung disease during the first 6 weeks of life, therefore they are unable to recapitulate the lung phenotype that is observed in humans.

### ***Zebrafish model***

The zebrafish CF model was produced using transgenic zebrafish mutant lines [115]. These animals were inexpensive to house and showed that CFTR channels respond to agonists and antagonists, similar to human CFTR. This model was able to demonstrate the importance of CFTR function in fluid secretion; however, the lung phenotype is not fully elucidated in this model.

### ***Porcine model***

Due to the expression of the CACC in mice, the CF pig model was developed because of their similar airway and lung anatomy to humans. Adeno-associated virus vectors that targeted the CFTR gene in fibroblasts from fetal pigs and somatic cell nuclear transfer of the cells into oocytes was used to generate CFTR KO piglets [108, 116, 117]. Interestingly, at birth, the CFTR KO piglets' lungs had no sign of pathology [118], however bronchioalveolar lavage fluid (BALF) from these piglets revealed a large number bacterial species [106, 118] that led to rapid lung infection, which was more severe than what was seen in human CF patients [106, 119]. Another problem with the pig model is that it is difficult to study the development lung disease because most of the CFTR KO pigs die from MI that is present in 100% of these pigs [106, 116, 118, 120, 121]. The

pig model was able to mimic many of the pathologies that is seen in human CF, however, only a small population of animals were used because of the difficulty to keep them alive, even after ileostomy or cecostomy to cure the MI problem [121, 122]. Thus, it would be beneficial for a new model to provide insight into the pathogenesis of CF.

### ***Ferret model***

CFTR KO ferrets were also developed by the same manner as the pig model due to similarities in lung function and architecture of that of human lungs [123]. The ferret model revealed similar lung pathologies as in humans in that there was air obstruction, thick mucus accumulation and inflammation [124]. Similar to what is seen in the pig model, CFTR KO ferrets developed spontaneous lung infections after birth, however the lung pathology was more severe than what is seen in human CF patients [124-127]. Like the pig model, CFTR KO ferrets developed MI at a higher percentage than humans with CF. These ferrets develop MI at an incidence of 50% to 100%, and they die within 36 hours due to intestinal obstruction and sepsis [108]. The animals that do survive the MI will eventually die because of malabsorption. A gut corrected model was also developed to correct MI in the ferret model, but once again there was difficulty in keeping the animals alive [125].

### ***Sheep model***

The sheep model has been used in studying many respiratory disease such as asthma and chronic obstructive pulmonary disease (COPD) due to their airways being similar to humans anatomically and functionally [128, 129]. Therefore, CFTR KO sheep were generated by using the CRISPR/Cas9 genome editing and somatic cell nuclear transfer methods [103]. Early reports suggest that the CFTR KO sheep demonstrate severe intestinal obstruction that is similar to human babies. However, the upkeep of the animal model is unfeasible, therefore a limited number of laboratories can use these animals.

## Conclusions

The pathogenesis of CF is still undeveloped, despite the many models at our disposal. Cell culture models have been critical in the development of preclinical trials, however, they are unable to recapitulate the disease pathophysiology of that can be seen in intact organs [130, 131]. The mouse model is unable to recapitulate the human lung phenotype, while the pig and ferret models have a more severe lung phenotype compared to humans. Also, the pig and ferret models are difficult to keep alive due to the severe intestinal obstructions, therefore studies can only be performed on few animals at a high cost. Therefore, a new model must be developed that recapitulates the human lung phenotype that can be studied without the worry of an early death. We report the generation and the characterization of the CF rabbit model. Table-1 illustrates and compares rabbits to other animals that have already been developed as major CF models. Rabbit CFTR consists of 1481 amino acids, similar to the 1480 amino acids for human CFTR. Rabbit CFTR has ~93% identity to human CFTR, the highest amongst the other animals used to generate CF animal models. With respect to disease pathogenesis, the rabbit lung has few, if any SMGs and has an architecture that is similar to human distal airways [132-138]. In this part of the study we characterize and determine the functional defect of CF rabbits' airway and lungs.

**Table 1: CFTR related characteristics among species**

Species	No. of amino acid	Identity to human (%)	CFTR Locus (Ch*)	Days of gestation	Avg. litter size	Sexual maturation	Avg. life expectancy (years)	SMG** / goblet cells	# of chromosome
Human	1480	100	7	280	1	10-16yr	~78	Yes/Yes	46
Mouse	1476	78	6	21	6	6-8 wks	2	Rare/Yes	40
Rat	1476	78	4	22	6	8wks	2-3	Yes/Yes	42
Pig	1482	92	18	114	10	6-8 months	10-15	Yes/Yes	38
Ferret	1484	91	?	42	8	4-6 months	8-10	Yes/Yes	40
<b>Rabbit</b>	<b>1481</b>	<b>93</b>	<b>7</b>	<b>30</b>	<b>8</b>	<b>4-6 months</b>	<b>8-10</b>	<b>Rare/Yes</b>	<b>44</b>

\* Ch: chromosome; \*\*SMG, submucosal gland

The overall goal of this project is to determine and delineate underlying mechanisms of the premature degradation of CFTR-F508del, and to determine if the absence of CFTR in rabbits is able to recapitulate airway and lung phenotypes seen in human CF patients. ***Our hypothesis is that RNF19B and UBE 2L6, proteins part ubiquitin proteasome system, are responsible for the degradation of F508del, and the absence of CFTR in the rabbit mimics what is seen in human CF airway and lung.***

### **Specific Aims**

#### ***Aim 1: Identify early checkpoints in the ubiquitin proteasome system that is involved in F508del degradation***

Previous studies have looked at the degradative machinery involved in CFTR degradation. However, the ER-resident E3 ligases may serve a role in the ER retained F508del degradation, therefore, uncovering these proteins and characterizing their role is crucial for understanding the degradation of F508del. Our preliminary data indicate that the E3 ligase, RNF19B and its interacting partner, the E2 conjugating enzyme UBE 2L6, is involved in F508del degradation. Using cell model systems, we will uncover the degradation of F508del by RNF19B and UBE 2L6 through siRNA experiments, overexpression experiments, cycloheximide-chase experiments, immunohistochemistry, biotinylation experiments, and functional experiments.

#### ***Aim 2: Determine the Functional Defect of CFTR Knockout rabbits' airway***

Understanding the molecular mechanism of CFTR degradation is important, however there are limitations in the *in vitro* system. Therefore, we used CRISPR/Cas9 gene editing to knockout (KO) the CFTR gene in the rabbit genome. We must characterize and confirm that this model mimics the phenotypes that is seen in human CF patients, especially the lung phenotype. Once this is accomplished, we will use this model to pursue pharmacologically targets that we find in the first aim. We will use electrophysiological, biochemical and pathological experiments on these animals to characterize our model.

### **CHAPTER 3: DEGRADATION OF CFTR-F508DEL BY THE E3 LIGASE RNF19B AND THE UBIQUITIN E2 CONJUGATING ENZYME UBE 2L6**

#### **Introduction**

CF is the most common, lethal autosomal recessive disease caused by a mutation in the gene encoding CFTR [7, 139]. CFTR is a cAMP regulated chloride channel that is a member of the ABC superfamily. The most common mutation amongst CF patients is the deletion of the phenylalanine residue at position 508 (CFTR-F508del). CFTR-F508del (F508del) is unable to achieve a native, folded state that is required for the protein to export from the ER to the apical membrane of epithelial cells [8]. F508del is synthesized in the ER, and it is trapped in the ER because it is unable to obtain its native state [15, 19, 20, 140]. It is polyubiquitinated, translocated to the cytosol and is eventually degraded by the 26S proteasome [9, 19, 141]. This network is generally called ERAD [66]. Studies have previously shown that F508del has a folding defect that can be adjusted by chemicals to promote proper folding and introducing channel function at the plasma membrane [9, 11, 19]. The ER folding pathway of CFTR is tightly coordinated with the ERAD pathway whereby misfolded CFTR are targeted to the cytosolic proteasome [142]. This is extremely important because pharmacological agents that may help with F508del folding or the blocking of its degradation may help CF patients.

A small amount of F508del can return to its proper folding pathway with the help of correctors, such as VX-809 [143, 144]. Experimental restoration of F508del trafficking to the plasma membrane results in partial function of the chloride channel, raising therapeutic speculations [9, 11]. The UPS is essential in the degradation of F508del. Ubiquitin is covalently attached to F508del by an isopeptide linkage between the c-terminal glycine of ubiquitin and amino group of lysine of the substrate (F508del). This is done through a cascade system, which consists of E1 activating enzyme, E2 conjugating enzymes, and E3 ligase enzymes [145]. Ubiquitination of F508del occurs when the E3 ligase binds to the F508del and E2 enzyme that is

thioesterified with ubiquitin [90, 146], and brings both to close proximity so that ubiquitin is transferred from the E2 to the substrate [21]. Ubiquitin E3 ligases are important enzymes that transfer ubiquitin from an E2 ubiquitin-conjugating enzyme to the mutant CFTR. E3 ligases are important for they show substrate specificity for ubiquitin transfer to the target proteins. To date, there are little studies in mammalian cells that identify E2 conjugating enzymes and ER-localized E3 ubiquitin ligases that function in the degradation of F508del.

About 60% of newly synthesized wild type-CFTR (WT-CFTR) and almost 99% of F508del is degraded by the UPS [17]. Therefore, there seems to be specific checkpoints set in place within the ER that allows F508del to stray apart from its WT counterpart during early stages of CFTR biogenesis. We believe that ER resident E3 ligases and there corresponding E2 conjugating enzymes are the initial checkpoint proteins that may be responsible for the divergence of WT-CFTR and F508del during CFTR biogenesis.

Previous studies have identified the E3 RMA1 and the E2, UBC6e cooperate to degrade both CFTR and F508del. [22, 24] However, there seems to be other mechanisms that facilitate F508del degradation because these studies still illustrate a significant amount of F508del that is being degraded, even when the above-mentioned proteins were silenced. The E2 UBCH5 forms an E3 complex with CHIP and the E3 ligase Hdj2 to ubiquitinate F508del [13, 20, 22]. When this complex is destroyed, F508del is still not able to traffic out of the ER, but instead is degraded. Therefore, other E2/E3 complexes may exist in F508del degradation and other mechanisms need to be sorted out to determine other potential therapeutic approaches to help prevent F508del degradation.

Through a literature search of E2 conjugating enzymes that seem to interact with ER membrane-bound E3 ligases, we discovered the E2 conjugating enzyme UBE 2L6, whom has its role in the ubiquitin conjugating pathway[147-149] This E2 interacts with RING E3 ligases that

are bound to the ER such as RNF122, RNF19B, and also RNF19A[150]. This is important because it has already been shown that certain E3 ligases, such as RMA1, acts in the ER membrane to identify the misfolded F508del [24]. We were able to determine that the E2 UBE2L6 was a key player in F508del degradation, and its interacting E3 ligase, RNF19B, also mediates F508del. In this study, we explore the possible roles of UBE 2L6 and the E3 ligase RNF19B in the proteasomal degradation of F508del. We determined that both proteins degraded F508del when overexpressed. Also, when both proteins were knocked down through siRNA-mediated silencing in HBE cells, there was an increase in expression of F508del, which was further enhanced when treated with VX-809. The same cells treated with VX-809 also had more chloride channel activity at apical membrane of the cells. Our results provide a clearer landscape of the molecular mechanism that underlies the proteasomal degradation of F508del through UBE 2L6 and RNF19B.

## **Methods**

### ***Antibodies and chemicals***

Mouse monoclonal anti-CFTR antibody was obtained from University of North Carolina at Chapel Hill. Rabbit polyclonal actin and polyclonal anti-NA/K ATPase were purchased from Cell Signaling. Mouse monoclonal UBE 2L6 antibody were acquired from Research Diagnostics Inc. Mouse monoclonal Myc, HA, and His-tag antibodies were bought from Abcam. VX-809 and MG132 were obtained from Selleck Chemicals, GlyH101 was obtained from Calbiochem, Forskolin, 3-Isobutyl-1-methylxanthine (IBMX) and cycloheximide (CHX) were purchased from Sigma. siRNA was purchased through Dharmacon Inc.

### ***Cell culture and drug treatment***

CFBE-F508del expressing cell line was established from CFBE41o<sup>-</sup> (CFBE), a well-characterized human airway epithelial cell line. CFBE cells was derived from the bronchial epithelial cells of a CF patient with *cftr* F508del/F508del genetic background and with no

detectable expression of the mutant protein. CFBE-F508del cells were cultured in MEM with 10% fetal bovine serum addition of 0.5  $\mu\text{g/L}$  puromycin. All cells were maintained in a humidified atmosphere containing 5%  $\text{CO}_2$  at 37  $^\circ\text{C}$ . Confluent cells were treated with VX-809 in culture medium at the designated concentration for 24 h. Cells were harvested after 24 h treatment. HEK 293 cells were cultured in DMEM with 10% fetal bovine serum.

#### ***Plasmid constructs, DNA constructs.***

F508del in pcDNA3.1 vector was described previously [26]. The UBE 2L6 and RNF19B cDNA sequence was amplified by PCR and inserted into pcDNA3.1(+) at EcoR1 and EcoRV sites. HA-ubiquitin was purchased from Addgene.

#### ***Immunoblotting***

Cells were lysed by sonication in lysis buffer (50 mM HEPES, 150 mM NaCl, 1 mM EDTA, 1% NP40, 10% glycerol and protease inhibitors cocktail). Specifically, protein samples were resolved by SDS-PAGE and transferred to PVDF membranes, which were blocked at room temperature for 1 h with 5% (w/v) non-fat milk in TBST (10 mM Tris (pH 8.0), 150 mM NaCl, 0.05% Tween 20). The blots were incubated with primary antibodies in TBST with 10% fetal bovine serum at room temperature for 2-3 h. The blots were then washed three times with TBST and incubated with horseradish peroxidase-conjugated secondary antibodies for 1 h, followed by three washes with TBST. The reactive bands were visualized by incubation with enhanced chemiluminescence substrates (PerkinElmer Products) and exposure to X-ray film (Eastman Kodak Co).

#### ***Co-immunoprecipitation (Co-IP) for ubiquitin assay***

Cell lysate treated with MG132 in Lysis buffer ( (50 mM HEPES (pH 7.4), 150 mM NaCl, 1 mM EDTA, 1% NP-40, 10% glycerol) was precleared with protein A/G-Sepharose beads (Invitrogen). The precleared lysate was mixed with 10ug of the indicated antibody and 25ul of

protein A/G-Sepharose beads and incubated overnight at 4°C with gentle rotation. Immunocomplexes were resuspended in SDS sample buffer and subjected to SDS-PAGE gel and immunoblotting.

### ***Cycloheximide (CHX) chase analysis***

After 24 h treatment with designated reagent, cells were continued to be cultured in medium supplemented with 50 µg/ml CHX and harvested at designated time points. Cell extracts were subjected to the immunoblotting analysis with appropriate antibodies.

### ***Biotinylation and pulldown of CFTR on streptavidin beads***

After treatment with specified reagent of 24 hours, cells were washed 3 times with PBS and exposed to 0.5mg/ml in PBS EZLink Sulfo-NHS-LC--biotin (Thermo Scientific) for 1 h on ice. Cells were washed 3 time with PBS, quenched with 100mM glycine in PBS, and rinsed 2 time again. Then cells were solubilized by sonication in RIPA buffer (150 mM NaCl, 1 mM Tris/HCl, 0.5% (w/v) deoxycholic acid, 1% (w/v) NP-40, 0.1% SDS, 2 mM EDTA, 50 mM NaF and protease inhibitors). The resulting lysate was centrifuged at 21100 g for 10 min at 4<sup>0</sup>C, and supernatant protein content was determined using protein assay dye reagent (Bio Rad). The supernatant was incubated with streptavidin beads for overnight at 4<sup>0</sup>C. After a brief centrifugation the supernatant was removed, the beads were washed 4 times with lysis buffer. Pull-downed proteins were resolved by SDS-PAGE, transferred to PVDF membranes and performed an immunoblot as described above.

### ***Ussing chamber experiments***

CFBE-F508del cells grown on collagen-coated transwell filters (Costar, 0.33 cm<sup>2</sup>, 0.4-µm pore) were polarized and treated with indicated reagent 24h. Filters were mounted in Ussing Chambers (Physiologic Instruments #P2300). The basolateral bathing solution consisted of 120 mmol/L NaCl, 25 mmol/L NaHCO<sub>3</sub>, 3.3 mmol/L KH<sub>2</sub>PO<sub>4</sub>, 0.8 mmol/L K<sub>2</sub>HPO<sub>4</sub>, 1.2 mmol/L

CaCl<sub>2</sub>, 1.2 mmol/L MgCl<sub>2</sub> and 10 mmol/L d-glucose. The apical bathing solution replaced 120 mmol/L NaCl with 120 mmol/L Na glutamate to achieve a transepithelial chloride gradient. The bathing solutions were maintained at 37°C and gassed with 95% O<sub>2</sub>, 5% CO<sub>2</sub> to retain a pH 7.4. Short-circuit current and transepithelial resistance were measured continuously using a voltage-clamp (VCC-MC8) and Acquire and Analyze v2.3 data acquisition hardware and software (Physiological Instruments, San Diego, CA, USA).

Filters were equilibrated for approximately 15 min to permit electrical parameters to stabilize, and baseline short circuit current (*ISC*) was measured. 10 μM forskolin and IBMX was added to the basolateral chamber to activate and remain CFTR-mediated anion secretion. After 3 min and currents had reached steady state 10 μM/L CFTR inhibitor Glyh 101 was added to the apical solution. Stop record after currents had achieved steady-state. Changes in short-circuit currents were calculated from the mean currents obtained during the 20-s period.

### ***Confocal microscopy***

Immunofluorescence staining of filter-grown cells was performed as described previously [26]. Briefly, CFBE-F508del cells were fixed in 4% paraformaldehyde and permeabilized with a mixture of 4% paraformaldehyde and 0.1% Triton X-100. The cells were then washed three times with buffer A (0.5% BSA and 0.15% glycine at pH 7.4 in phosphate-buffered saline). After blocking with purified goat serum, the monolayers were incubated in the appropriate primary antibodies (anti-Myc 1: 300, and anti-CFTR217 1:300) for 1 hour followed by three washes in buffer A and subsequent incubation with fluorescein isothiocyanate (green) or rhodamine (red)-labeled secondary antibodies (1:1000, Molecular Probes) for another hour. After washing with buffer A, the filters were mounted on glass coverslips using synthetic resin and subjected to confocal microscopy. Collected images were exported to ImageSpace (Molecular Dynamics) for subsequent reconstruction and processing.

### ***Quantitative real-time reverse transcription PCR analysis***

Total cellular RNA was extracted using TRIzol reagent and reverse-transcribed to cDNA using a random primer. The real-time PCR reaction mixture containing cDNA template, primers and SYBR Green PCR Master Mix (Invitrogen) was run in a 7,500 Fast Real-time PCR System (Applied Biosystems). Fold changes of mRNA levels were determined after normalization to internal control of  $\beta$ -actin RNA levels [151]. RNF19B Forward primer: TGCATGACTCAGCAAAGTGGA. RNF19B Reverse primer: GCATGAACATGGAGCGAGTCC

### ***Data analysis***

The immunoblot images were scanned at 600 dpi for densitometry analysis using Image J software. The Values are means  $\pm$  SEM. Statistical significance of differences was determined using paired two-tailed Student's t-test.

## **Results**

### ***RNF19B is a candidate in F508del degradation***

To identify which ER resident E3 Ligase maybe involved F508del degradation, we performed a siRNA screen on ER resident E3 ligases on HBE cells (Figure 1A, 1B). The screen illustrated that RNF19B, when knocked down, increased the expression of F508del. Therefore, we determined that RNF19B may be a candidate in F508del degradation [152]. RNF19B is a Ring finger protein family of E3 ligases, which interacts with E2 conjugating enzyme(s) and substrates, facilitating the transfer of an activated ubiquitin to the substrate [153, 154]. RING finger E3 ligases have a RING structure that is involved in ubiquitinating its substrate. To show that this site is involved in ubiquitinating F508del, we generated a catalytically non-functioning RNF19B RING mutant where we mutated a cysteine residue at position 119 to a serine residue (c119s) to disable the RING domain. HEK 293 cells were co-transfected with F508del

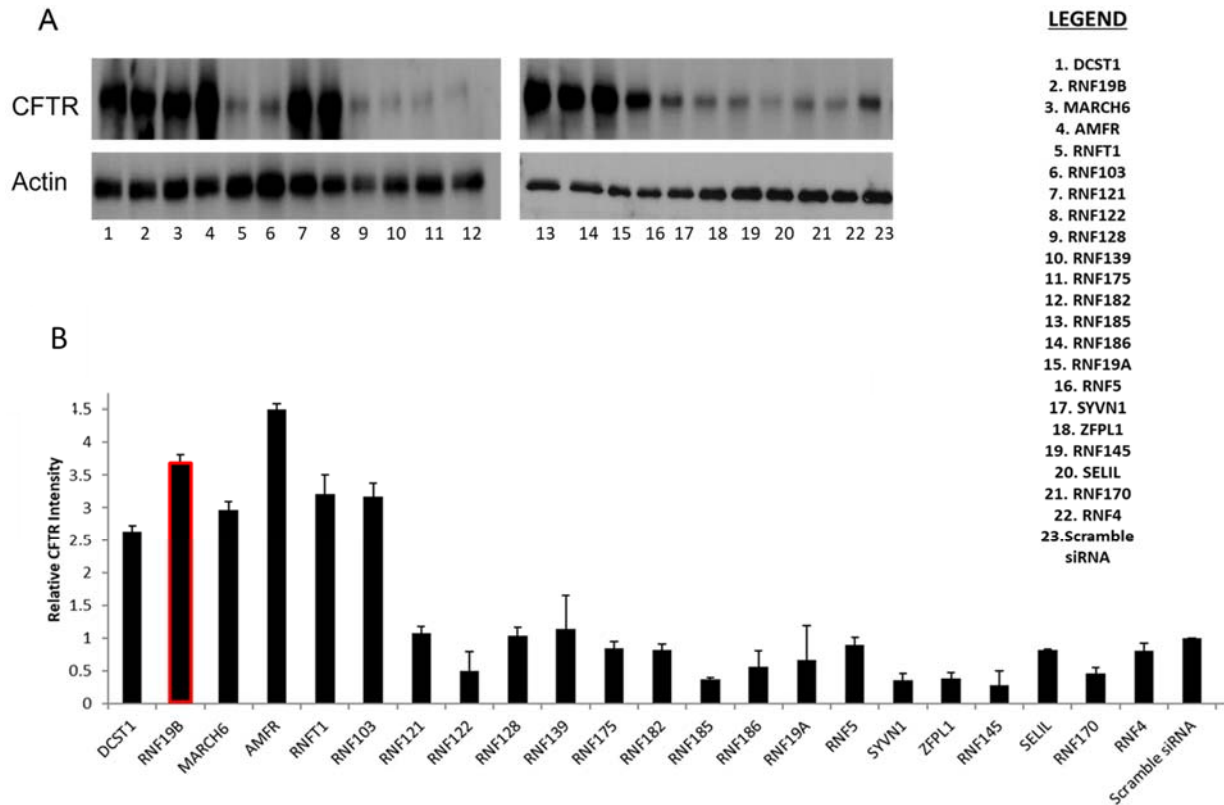


**Figure 1. E3 ubiquitin ligase siRNA library screen:** **A.** HBE cells, CFBEF508del cells, were transfected with 30 nM of the indicated siRNA. The blot shows CFTR B-band expression. **B.** Quantification of CFTR B-Band/Actin intensity of the E3 ligase siRNA screen (mean  $\pm$  SE,  $n = 3$ ,  $p < 0.05$ ).

and with Myc-RNF19B or with Myc-RNF19B c119s (Figure 2A). Overexpressing Myc-RNF19B causes F508del degradation. When transfected with the catalytically non-functioning mutant, Myc-RNF19B c119s, F508del is expressed to similar levels as control (Figure 2A, 2B). To determine if RNF19B ubiquitinates F508del, HEK293 cells were first transfected with F508del and with Myc-RNF19B plasmid. 24 hours post-transfection, HA-ubiquitin was transfected into these cells. The cells were then harvested and CFTR was pulled down (Figure 2C). The left panel demonstrates that there is more HA-ubiquitin immunoprecipitated with F508del when RNF19B was overexpressed compared to control. The right panel demonstrates that total CFTR was the same between both conditions under MG-132 treatment. If RNF19B regulates F508del, they should be located in the same compartment. To determine if these proteins are localized within the same area of the cell, CFBE-F508del cells were

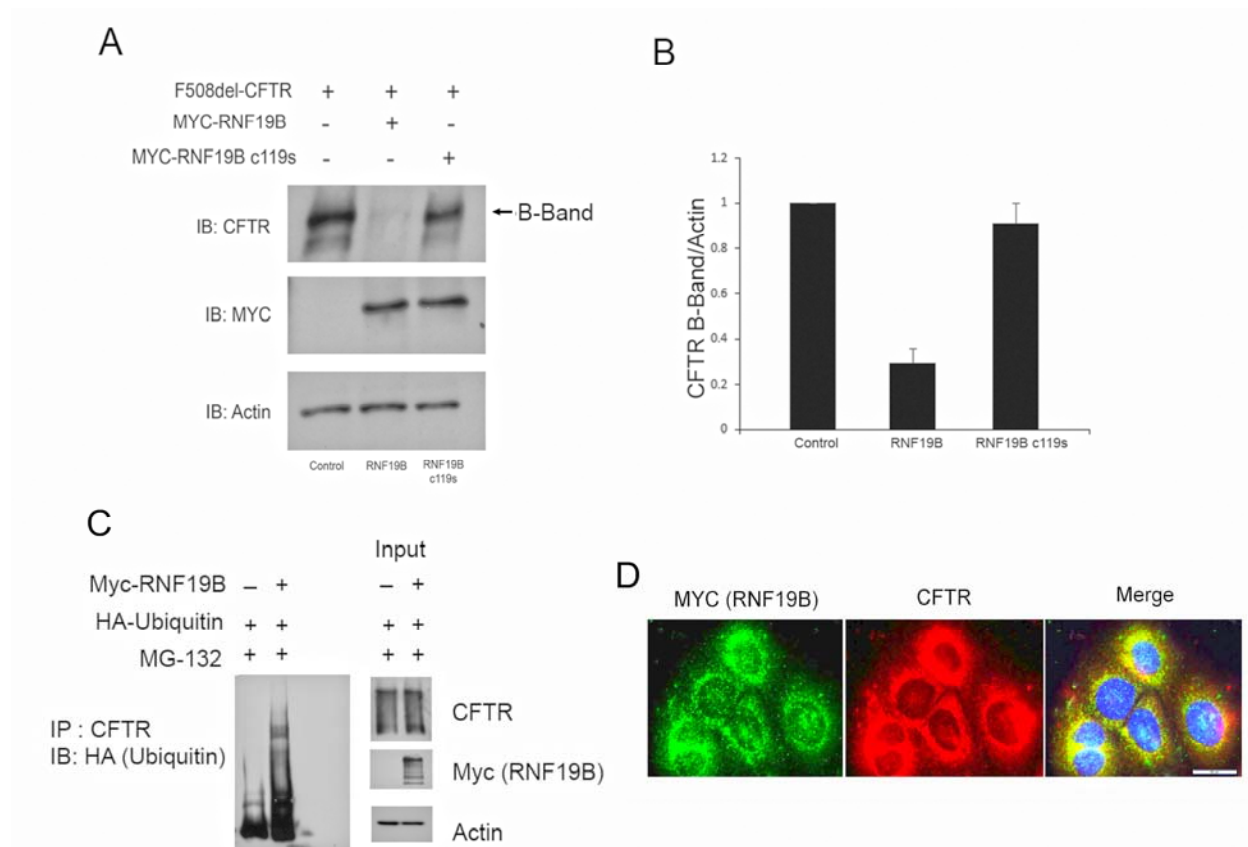


**Figure 2. RNF19B ubiquitinates F508del and colocalizes with F508del in the ER.** Stable HEK293 cells were co-transfected with F508del and with either Myc tagged RNF19B or Myc tagged RNF19B mutant (RNF19B c119s). **B.** Quantification of panel A. **C.** HEK 293 cells were transfected with F508del plasmid and control or Myc-RNF19B plasmid. 24 hours later, these cells were transfected with HA-Ubiquitin. Cells were harvested and CFTR (217) was immunoprecipitated. HA-ubiquitin was immunoblotted. Input was immunoblotted with the indicated antibodies. Conditions were all under MG132 treatment. (mean  $\pm$  SE,  $n = 3$ ,  $p < 0.05$ ) **D.** F508del-CFBE cells were transfected with Myc tagged RNF19B and immunostained for Myc (**green**) and F508del (**red**). Nuclei were stained blue. Scale bar 50  $\mu$ m.

transfected with Myc-RNF19B and then immunostained with Myc (green) and F508del (red) (Figure 2D). The immunostaining shows that Myc-RNF19B is localized with F508del in the perinuclear area, which is indicative of the ER. To determine how RNF19B affects the half-life of F508del, we performed a cycloheximide-chase where HEK 293 cells were co-transfected with F508del and with the control or with Flag-RNF19B for 48 hours. The cells were then treated with 50 $\mu$ g/ml cycloheximide for the different indicated time periods. (Figure 3A, 3B). Overexpressing RNF19B decreased the half-life of F508del from 60 minutes to about 20 minutes, suggesting RNF19B participates F508del degradation.

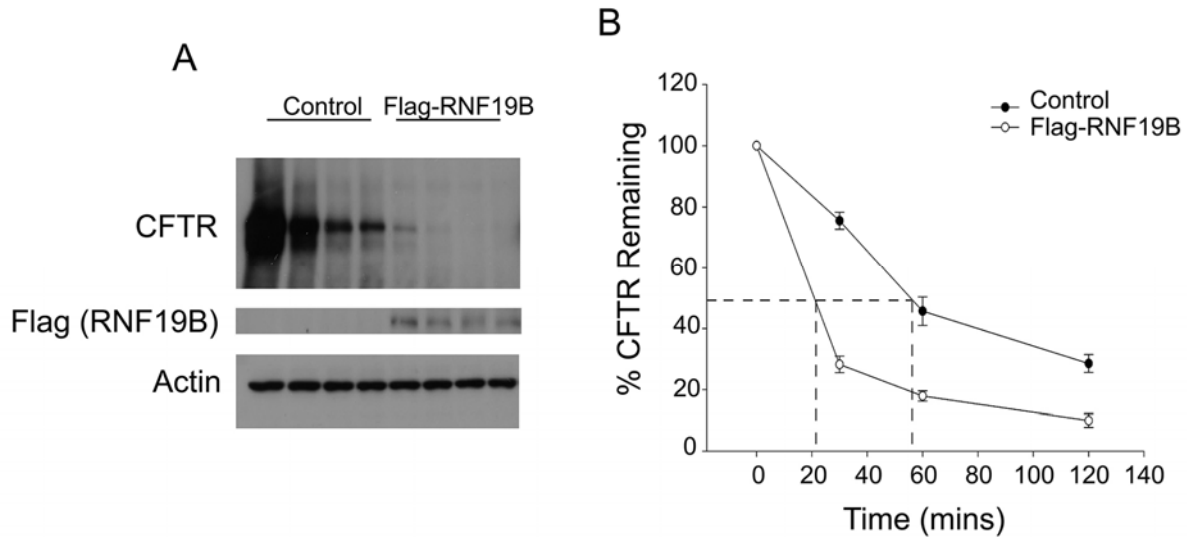


**Figure 3. RNF19B over-expression accelerates F508del-CFTR degradation.** **A.** Cyclohexamide (CHX) experiments were performed on HEK 293 cells co-transfected with F508del and with a control or with Flag tagged RNF19B for 48 hours. The cells were then treated with CHX (50  $\mu$ g/ml) for the indicated times. **B.** The level of remaining F508del at different time points was quantified as the percentage of initial F508del level (0 min of CHX treatment). RNF19B expression resulted in a shorter half-life of F508del. (mean  $\pm$  SE,  $n = 3$ ,  $p < 0.05$ ).

### *Silencing RNF19B in HBE cells rescues F508del*

To determine if RNF19B has any effect on F508del, CFBE-F508del cells were transfected with siRNA against RNF19B. When knocking down RNF19B, there is an increase in F508del protein expression almost 3-fold (Figure 4A). Due to the lack of a sufficient antibody to RNF19B, silencing of RNF19B expression was confirmed by RT-PCR (Figure 4B). We overexpressed a Myc tagged RNF19B (Myc-RNF19B) plasmid into CFBE-F508del cells and transfected these cells with siRNA against RNF19B (Figure 4C, 4D) to determine knockdown of RNF19B in HBE cells. The knockdown of RNF19B increased endogenous F508del by about 3-fold in CFBE-F508del cells (Figure 4C, 4D). Next, HEK 293 cells were co-transfected with Myc-RNF19B and F508del (Figure 4E). 0.5  $\mu$ g of RNF19B decreases F508del by about 1.4-fold, whereas transfection with 1.0  $\mu$ g of RNF19B decreases F508del by about 4.7-fold (Figure 4E, 4F), indicating RNF19B degrades F508del in a dose-dependent manner.

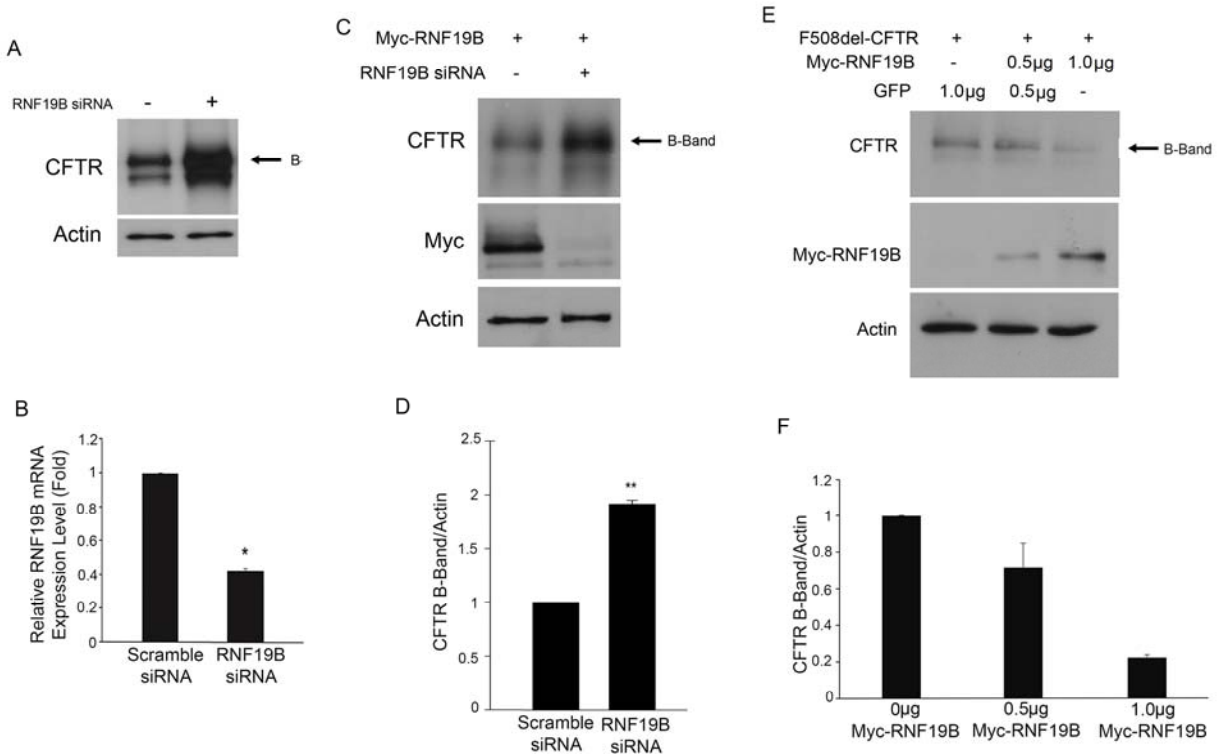


**Figure 4. Silence of RNF19B increased F508del Expression and RNF19B mediates F508del degradation in a dose-dependent manner** **A.** Silence of endogenous RNF19B expression using siRNA increased F508del expression by about 3-fold in CFBE-F508del cells. **B.** Quantification of mRNA expression levels of RNF19B in CFBE-F508del cells with RNF19B knocked down using siRNA. **C.** Silence of overexpressed RNF19B expression using siRNA increased endogenous CFTR-F508del by approximately 3-fold in human airway epithelial cells. **D.** Quantification of panel C. **E.** HEK293 cells were stably transfected with Myc-tagged RNF19B. **F.** Quantification of CFTR-F508del expression level from panel E. (mean  $\pm$  SE,  $n = 3$ , \* =  $p < 0.05$ , \*\* =  $p < 0.01$ ).

***F508del function is enhanced by RNF19B knockdown in the presence of VX-809 treatment***

To further determine if RNF19B is involved F508del degradation and its function, we needed to determine if CFTR trafficking to the plasma membrane is affected by RNF19B. We performed biotinylation experiments to determine if more F508del traffics to the plasma membrane when RNF19B is silenced (Figure 5A). Knockdown of RNF19B promotes F508del C-

band to the plasma membrane to act as a chloride channel. When RNF19B is knocked down with

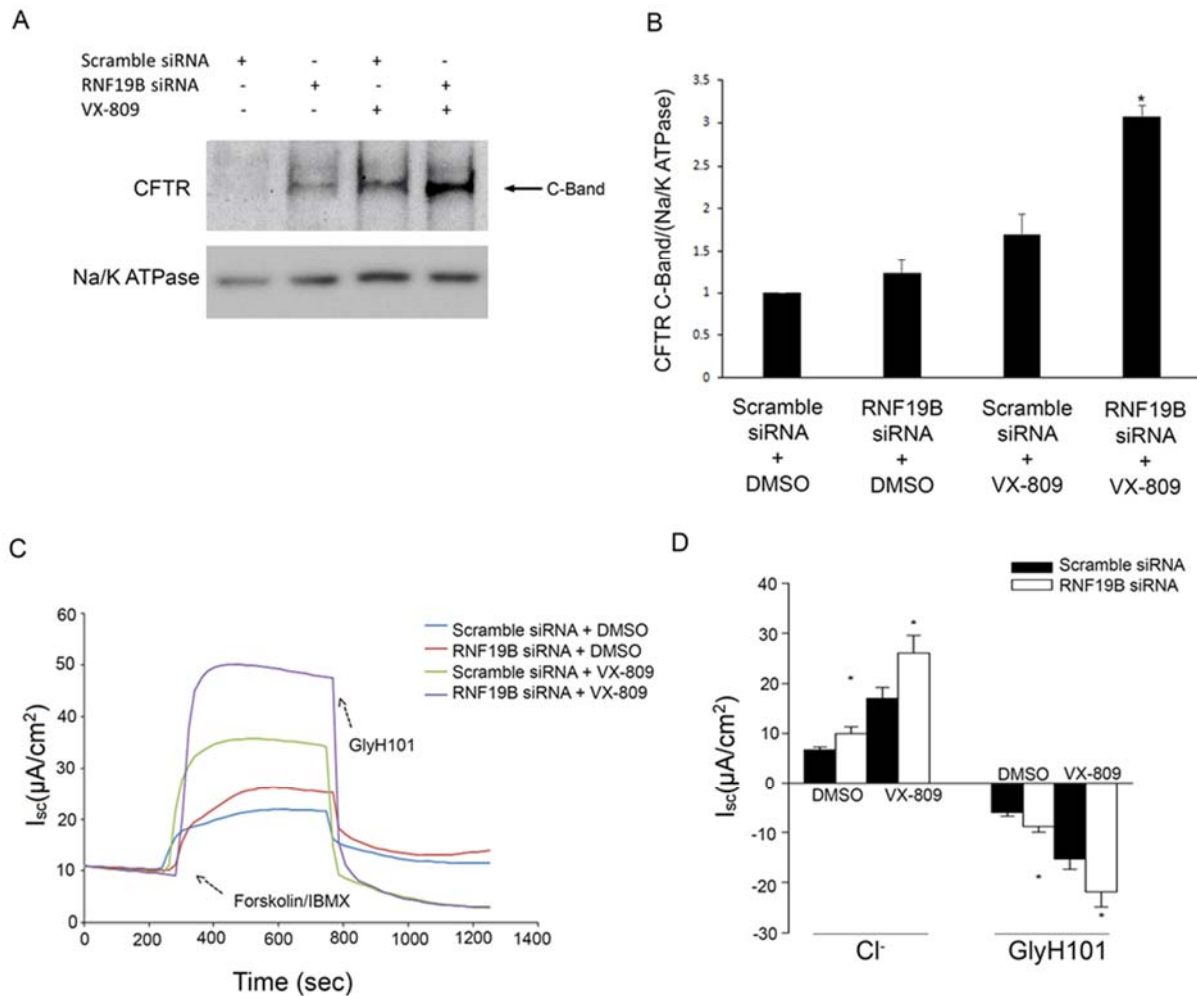


**Figure 5. Silence of RNF19B promotes VX-809-mediated F508del trafficking to the plasma membrane and enhances F508del-CFTR function.** **A.** Biotinylation experiment illustrating that silencing endogenous RNF19B in CFBE-F508del cells using siRNA increased F508del C-band expression to the plasma membrane compared to control and even more so with 3 $\mu$ M VX-809 treatment. **B.** Quantification of panel A. **C.** Ussing Chamber experiments. CFBE-F508del cells were first treated indicated siRNAs for 48hrs and then incubated with 3  $\mu$ M VX-809 for additional 24 hrs in 6.5 mm transwells. Short-circuit currents were retrieved through the Ussing chamber and F508del currents were determined through the treatment with the indicated conditions. Forskolin/IBMX (10 $\mu$ M) and GlyH101 (10 $\mu$ M). **D.** Quantification of short-circuit currents. (mean  $\pm$  SE,  $n = 3$ ,  $p < 0.05$ ).

VX-809 treatment, there is a 1.8-fold increase in C-Band (Figure 5A, 5B). To determine if there is enhanced F508del function when RNF19B is knocked down, we performed Ussing Chamber experiments. We transfected CFBE-F508del cells with siRNA against RNF19B or a scramble

siRNA as a control. 48 hours post-transfection, we treated the cells with either 3  $\mu$ M VX-809 or with DMSO for 24 hours. 24 hours post-treatment, cells were set up in the Ussing chamber to measure short-circuit currents. Short-circuit currents demonstrated that compared to control, RNF19B knocked down in CFBE-F508del cells increased short-circuit currents by about 3.25  $\mu$ A/cm<sup>2</sup> compared to scramble controls when stimulated by forskolin and IBMX (Figure 5C, 5D). There is an increase of about 7.7  $\mu$ A/cm<sup>2</sup> in CFTR function when CFBE-F508del cells have RNF19B knocked down and treated with VX-809 compared to scramble control (Figure 5C,5D). This set of data indicates that there is rescue F508del protein and function when RNF19B is silenced in HBE cells.

#### ***Overexpressing UBE 2L6 degrades F508del***

Through a literature search, we were able to discover UBE 2L6 interacts with many E3 ligases that were found in the ER [150]. Interestingly, through the literature search we were able to determine that RNF19B is a partner of UBE 2L6 [152]. This interaction with E3 ligases in the ER may mediate F508del degradation; therefore we wanted to observe what happens to CFTR when we overexpress UBE 2L6. We used HEK 293 cells and co-transfected with F508del and UBE 2L6 for 48 hours. 48-hours post-transfection, total protein lysates were harvested and probed for F508del levels by immunoblot analysis. Overexpressing UBE 2L6 decreased F508del expression by about 2.5-fold (Figure 6A, 6C).

To further confirm UBE 2L6 effects on degrading F508del, we developed a dominant-negative mutant of UBE 2L6 where a cysteine residue at position 86 was mutated to a serine residue (UBE 2L6 DN). This mutation will destroy the catalytic activity of UBE 2L6 and therefore the activated ubiquitin is not able to transfer onto the E2. Hence, theoretically the ubiquitin is not able to transfer to the misfolded protein. We transiently transfected HEK 293 cells with F508del and with UBE 2L6 or UBE2L6 DN or a control (pCMV $\beta$ ) (Figure 6B). Consistent to previous

finding, overexpressing UBE 2L6 decreases F508del. When UBE 2L6 DN is overexpressed, F508del expression increases 1.9-fold (Figure 6B, 16C). These data suggest that UBE 2L6 facilitates F508del degradation by ubiquitination.

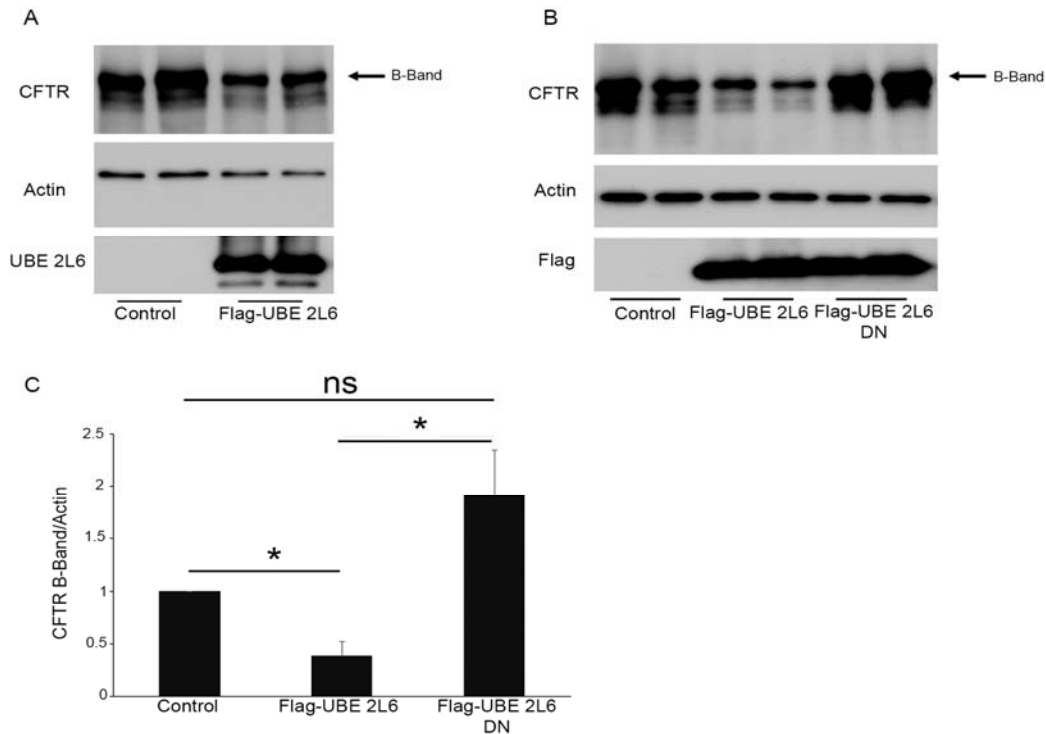


**Figure 6. UBE 2L6 over-expression increase F508del degradation.** **A.** HEK 293 cells were co-transfected with CFTR-F508del and control or Flag-UBE 2L6 plasmid. Cell lysates were subjected to immunoblot. Compared to the control, UBE 2L6 overexpression increased F508del degradation. **B.** HEK 293 cells were co-transfected with F508del and the plasmids that are listed above. Cell lysates were subjected to immunoblot. Compared to control, UBE 2L6 increased F508del. The dominant negative mutant, Flag-UBE 2L6-DN, decreased F508del degradation. Flag-UBE 2L6-DN plasmid was developed by mutating the cysteine at position 86 to a serine. **C.** Quantification of CFTR C-Band/Actin when Flag-UBE 2L6 or Flag-UBE 2L6 DN is overexpressed. (mean  $\pm$  SE,  $n = 3$ ,  $p < 0.05$ ).

### ***Silencing UBE 2L6 in HBE cells with VX-809 rescues F508del***

We next wanted to determine if we can rescue F508del if we silenced UBE 2L6 in human bronchiole epithelial (HBE) cells. We used cystic fibrosis HBE cells that have the F508 mutation (CFBE-F508del) and knockdown UBE 2L6 with siRNA. 48 hours post-transfection, the cells were treated with VX-809 or with DMSO as a control for 24 hours. VX-809 is a drug used in the CF field that folds F508del so that the protein is to traffic to the plasma membrane [143]. 24 hours

post-treatment, the cells were harvested and probed for CFTR and actin. When UBE 2L6 was knocked down with siRNA, there is a 2.8-fold increase in F508del expression, which is illustrated as Band-B (Figure 7A, 7C). Band B is the misfolded CFTR that is trapped in the ER where it will be eventually degraded by the proteasome in the cytosol. Interestingly, with VX-809 treatment, there seems to be a 2.7-fold increase in C-band expression of CFTR compared to control (Figure

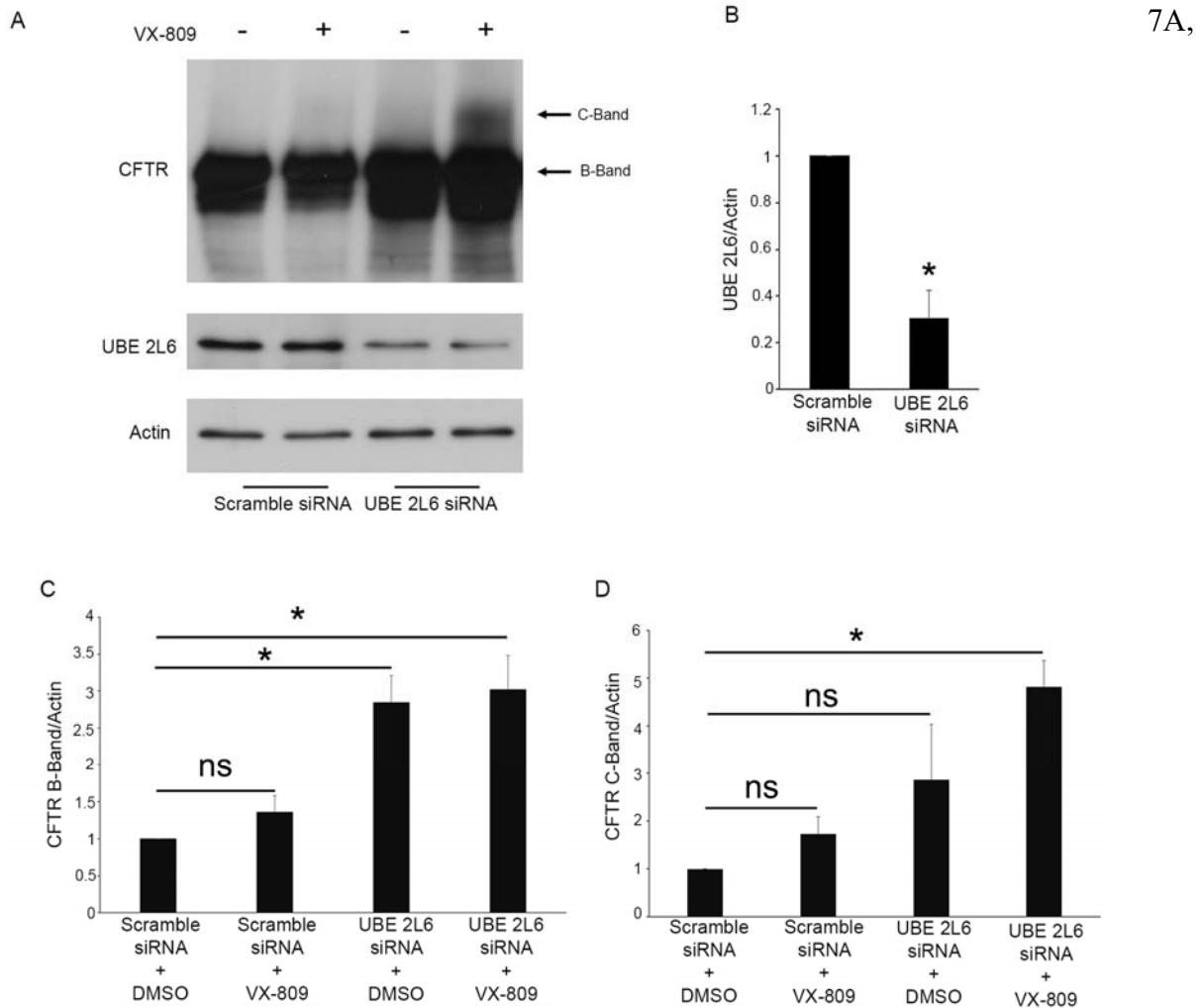


**Figure 7. Silencing UBE 2L6 in F508del-CFBE cells decrease F508del degradation. A.** Represented blot shows silencing of endogenous UBE 2L6 expression using siRNA in cells CFBE-F508del following 3  $\mu$ M VX-809 treatment increased immature F508del (B band) and rescued mature F508del-CFTR (C Band). **B.** Quantification of knockdown of UBE 2L6. **C.** Quantification of CFTR B-Band/Actin when UBE 2L6 is knocked down with or without VX-809 treatment. **D.** Quantification of CFTR C-Band/Actin when UBE 2L6 is knocked down with or without VX-809 treatment. (mean  $\pm$  SE,  $n = 3$ ,  $p < 0.05$ ).

7D). This is critical in that this shows that with UBE 2L6 knocked down, there seems to be a greater pool of B-band CFTR. With this increased pool of B-band, VX-809 helps more F508del to traffic to the plasma membrane.

***F508del function is increased with UBE 2L6 knockdown and VX-809 treatment***

To investigate how UBE 2L6 affect CFTR function, we used the Ussing chamber to measure F508del function by measuring forskolin-stimulated short-circuit current in HBE cells. We transfected CFBE-F508del cells with siRNA against UBE 2L6 or a scramble siRNA as a control. 48 hours post-transfection, we treated the cells with either 3  $\mu$ M VX-809 or with DMSO for 24 hours. 24 hours post-treatment, cells were set up in the Ussing chamber to measure short-circuit currents. A representative trace of the short-circuit currents demonstrates that compared to control, UBE 2L6 knocked down in CFBE-F508del cells, there is a slight, but significant increase in CFTR function by about 2.9  $\mu$ A/cm<sup>2</sup> when stimulated by forskolin and IBMX (Figure 8A, 8B). When CFBE-F508del cells have UBE 2L6 knocked down and treated with VX-809, there is an increase in CFTR function by about 5.4  $\mu$ A/cm<sup>2</sup> compared to cell transfected with scramble siRNA

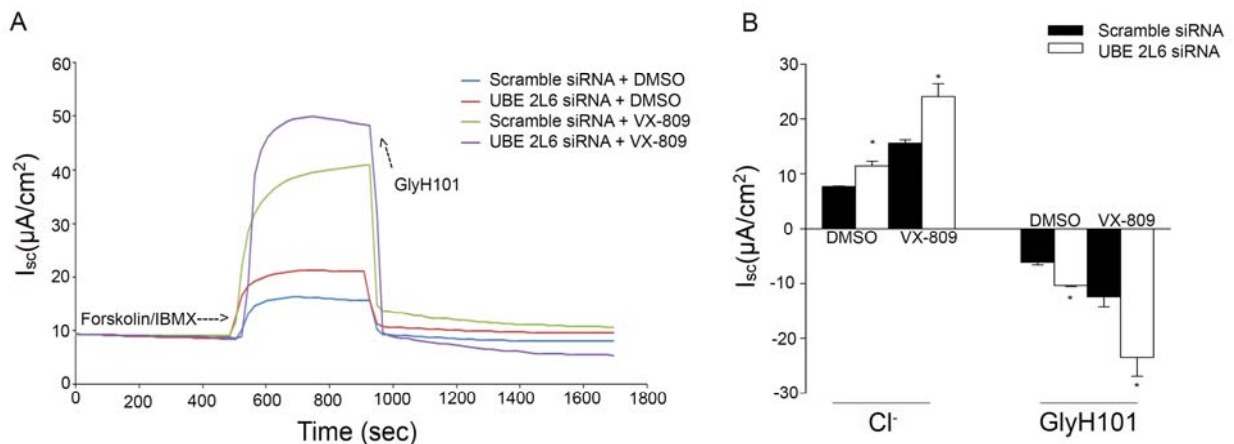


**Figure 8. UBE 2L6 knockdown enhances F508del function.** **A.** Ussing Chamber experiments. CFBE-F508del cells were first treated indicated siRNAs for 48 hrs and then incubated with 3  $\mu$ M VX-809 for additional 24 hrs in 6.5 mm transwells. Short-circuit currents were retrieved through the Ussing chamber and F508del currents were determined through the treatment with the indicated conditions. Forskolin/IBMX (10  $\mu$ M) and GlyH101 (10  $\mu$ M). **B.** Quantification of short-circuit currents. (mean  $\pm$  SE,  $n = 3$ ,  $p < 0.05$ ).

and treated with VX-809 (Figure 8A, 8B). The quantification of three experiments illustrates that knockdown of UBE 2L6 and VX-809 treatment had a significantly greater increase in F508del function compared to controls (Figure 8B).

## **Discussion**

Here, we have identified an E2 conjugating enzyme, UBE 2L6 that mediates the proteasomal degradation of F508del. We've found that when UBE 2L6 is knocked down in human airway epithelial cells and treated with VX-809, there is an increase in expression of CFTR C-band, the functional form of CFTR. UBE 2L6 works as a conjugating enzyme, acting as a transient holder of activated ubiquitin to be ready to tag a substrate [155], in this case misfolded F508del. We have shown that by mutating UBE 2L6 so that it cannot carry that activated ubiquitin, there is an increase in expression of F508del, therefore demonstrating that UBE 2L6 does indeed mediate the degradation of F508del through the ubiquitin proteasome system. Also, this shows that UBE 2L6 is an important player in the F508del degradation because the mutation to UBE 2L6 rescues F508del to similar levels as seen in control. Therefore, there is a greater pool of F508del that can be used on by VX-809 to allow for greater trafficking of the misfolded protein to the plasma membrane. Future studies will be focusing on developing and discovering small inhibitors to act as a drug to inhibit UBE 2L6 function so that there is a greater pool of F508del protein for VX-809 to act on. VX-809 will help fold F508del so that it can traffic to the plasma membrane.

With the increase in F508del pool, we also showed that there is an increase in CFTR function when UBE 2L6 is knocked down. Using human airway epithelial cells, we knocked down UBE 2L6 and determined that there was an increase in CFTR function when forskolin and IBMX was added to the cells. Importantly, when the same cells that had UBE 2L6 knocked down were treated with VX-809, there was a greater CFTR function compared to control. These experiments further support the idea that when UBE 2L6 is knocked down there is a greater pool of CFTR protein

that VX-809 can work on. Interestingly, previous studies have shown that UBE 2L6 conjugates with valosin-containing protein (VCP) during aberrant protein turnover [156]. VCP is a key component of the ERAD system, forming the Derlin-1/VCP/VIMP complex [81, 157]. VCP recognizes and process ubiquitinated substrates with cofactors such as p47, and UBXD1 [158-160]. The ATP-driven unfolding activity of VCP provides the force to extract substrates out of the ER membrane so that they can be degraded by the proteasome. We have already shown that VIMP, a linker between Derlin-1 and VCP in the ERAD complex, utilizes an E3 ligase, RNF5 to direct F508del for proteasomal degradation [161]. RNF5 interacts with the E2 conjugating enzyme Ubc6e to degrade F508del, not UBE 2L6.

We have also shown that RNF19B, an E3 ligase that interacts with UBE 2L6, mediates the degradation of F508del. Interestingly, RNF19B is localized in the endoplasmic reticulum [162, 163], where F508del is localized. Our data also demonstrates that VX-809 treatment RNF19B knocked down in HBE cells, there is an increase in F508del function at the plasma membrane. This is similar to what was seen when performing similar experiments with UBE 2L6. This is important in that not only does UBE 2L6 aids in the degradation of F508del, but that it interacts with and ER localized E3 ligases to assist in this degradation. Therefore, this is a potential early checkpoint in CFTR degradation because these two proteins that are involved in the ubiquitin proteasome system prevent F508del from trafficking to the plasma membrane to act as a chloride channel. If we are able to use small inhibitors to prevent these proteins from ubiquitinating F508del, we will be able to provide the cell with greater pool of F508del that is not degraded by the proteasome but allow VX-809 to act on more F508del so that it is able to traffic to the plasma membrane. Synergy between the knockdown of UBE 2L6 and RNF19B with VX-809 treatment, which enhanced F508del chloride secretion, indicates that these two proteins may offer a

therapeutic approach for CF. This allows for more chloride channels to the plasma membrane that will be extremely beneficial to CF patients.

Previous studies have shown that RMA1 and Ubc6e are involved in the proteasomal degradation of F508del [24]. There have been other E3 ligases that have been implicated in F508del degradation including CHIP, gp78, Hrd1, Nedd4-2, and RNF185[95-99]. RNF5 acts to degrade F508del contrantranslationally, while CHIP acts posttranslationally [24]. RNF19B is homologous, structurally to RNF5, therefore we predict that RNF19B, with its interacting partner UBE 2L6, also degrades F508del contrantranslationally, however further studies are needed to confirm this. Based on the data presented, we propose the following mechanism that is involved by F508del degradation. Quality control checkpoints within the ER senses the misfolded F508del due to the F508del mutation. The misfolded F508del is brought into association with RNF19B and UBE 2L6 where both the E3 and E2 proteins cooperate to ubiquitinate F508del. The ubiquitinated F508del is then signaled to proceed to the proteasome for degradation.

F508del the most common mutation amongst CF patients, where these patients lack the functional form of CFTR to act as an anion channel[1]. With this mutation, therapeutic strategies that create the mature form of CFTR partially restores the function of CFTR at the apical membrane of cells. Previous work in our lab have shown that with VIMP knockdown significantly enhances the rescue effect of CF corrector VX-809[161]. This was similar to what was seen in this current study when RNF19B and UBE 2L6 were knocked down. Previously, CF therapeutic discovery was governed by a one-step rule, where chemicals were discovered either as a corrector for mutated CFTR or as an activator or inhibitor to increase or decrease CFTR-associated protein expression [164-167]. With the expansion of classification of CFTR mutation, and with our study, we suggest a two-step rule: First, prevent F508del from ERAD. Second, help the rescued F508del to fold and migrate to the cell surface to function as a chloride channel. This study presents

RNF19B and UBE 2L6 as potential targets for preventing early degradation of F508del, which may be important in the development of efficient therapies to treat CF.

## CHAPTER 4: FUNCTION DEFECT OF CFTR ABSENCE IN RABBITS

### Introduction

Mutations of *cftr* gene lead to cystic fibrosis (CF), one of the most common life-threatening autosomal recessive disorders in Caucasian population [28]. The disease is unique because it affects multiple organs with lung dysfunction contributing the most of the morbidity and the mortality [168-171]. There have been major progress in the understanding of CF pathogenesis since CFTR gene was cloned in 1989; however, many important questions remain unanswered [7]. Animal models are extremely demanded to understand human diseases CF animal models have undoubtedly contributed to the understanding CF pathogenesis and to test and develop therapeutic reagents, yet the existing models have their limitations, either because the animal models fail to reproduce major phenotypes observed in CF patients [102] or because the animal models are of very high maintenance costs and special animal cares [108].

In this study, we report the generation and characterization of rabbit models of CF, in consideration that human and rabbit share considerable anatomical and physiological similarities [132]. The amino acid sequence of rabbit CFTR has approximately 93% identity to that in human, which is the highest among all animals utilized to generate CF animal models. Our work show that disruption of CFTR gene in rabbits produces human-like Cystic Fibrosis rabbits which include spontaneous lung infections. The CF rabbit models may serve as a useful tool for this devastating disease.

Dr. Xu's lab at the University of Michigan developed a robust CRISPR-Cas9 based gene-editing platform in rabbits. To produce CFTR knockout (KO) rabbits, they first designed sgRNAs based on the CFTR exon 11 sequence. They tested the targeting efficiency of five different sgRNAs (sg-01 to -05) *in vitro* by microinjecting the different amount of individual sgRNAs and Cas9 RNA to pronuclear stage embryos and analyzed the editing efficiency using the blastocysts.

Among the five sgRNAs tested, sgRNA-02 was found the most effective. They next used sgRNA-02 for microinjection and performed embryo transfer. 162 embryos were transferred to 6 recipients, 11 live kits were obtained, and 3 kits were confirmed as CFTR F0 KO founders. The data presented here were from CF rabbits with one nucleotide deletion, which generated the stop codon at amino acid position 478.

## **Methods**

### ***Statement of animal care and use***

All animal maintenance, care and use procedures were reviewed and approved by the Institutional Animal Care and Use Committee (IACUC) of Wayne State University (WSU), the University Committee on the Use and Care of Animals of the University of Michigan. Rabbits were generated at the UM and Wayne State.

### ***Production of CFTR mutant rabbits***

Dr. Xu's lab at the University of Michigan developed a robust gene-editing platform in New Zealand White rabbits based on CRISPR/Cas9 [172-174]. Using this system, embryo microinjection followed by embryo transfer was performed to produce 3 CFTR mutant founder rabbits. Off-target effects of the guide RNA (sgRNA-02) in all three founders were tested by PCR amplification of the top 20 potential off-target sites. Upon sexual maturation (5-6 months), F0 mutant founders were bred with wild-type (WT, *i.e.*, *CFTR*<sup>+/+</sup>) animals to establish the F1 generation of heterozygous (*CFTR*<sup>+/-</sup>) rabbits. F1 animals were then inbred to obtain *CFTR*<sup>-/-</sup> ("CF") rabbits. Confirmation of CFTR knock-out was tested by electrophysiology, immunohistochemistry, and Western blotting.

### ***Animal husbandry***

The animals utilized in this study were produced at two locations, primarily to monitor electrophysiology and improve animal husbandry. At two weeks of age, the dam and kits were

given Golytely (an osmotic laxative, Braintree Labs, Braintree MA) to drink rather than water. The CF rabbits consumed this laxative for their entire life. At 4 weeks of age all kits were given Bioserve (Bio-Serve, Frenchtown, N.J.) in a bowl 2x/day as a supplement in addition to their regular rabbit chow (Teklad Global rabbit diet(230), Envigo, Madison WI). At weaning, the CF kits were given Bioserve in a bowl 1x/day as a supplement for their entire life. At 1 week of age all CF rabbits are weighed and abdominally palpated every other day for abdominal masses. If masses were detected, rabbits were treated twice a day with: 1) 50ml SQ warmed physiological saline; 2) PO 0.5 mg/kg cisapride (increases motility of lower gut; 3) PO 0.5ml/kg simethicone (anti-gas agent); 4) PO 0.5 mg/kg metoclopramide (increases motility of small bowel); and 5) PO 0.5 ml/kg lactulose (a laxative). Treatment continued until masses resolved. NOTE: Some of the older CF rabbits presented multiple times with gut symptoms which were reversed with our treatment protocol.

### ***Animal phenotyping***

Survival analyses was conducted by careful monitoring of animal mortality across time. In general, histological analyses were conducted using tissue collected in 10% neutral formaldehyde solution followed by paraffin embedding and staining (details in figure legends). Special stains are provided in the figure legends. The lung phenotype was further characterized by collection of bronchoalveolar lavage fluid followed by bacterial culture and cytology. The microbiome of selected samples was monitored by 16S RNA sequencing. Short-circuit current recordings in Ussing chambers were conducted on tracheal preparations [175-177].

### ***Immunoblotting***

Fresh lung tissues of CF and WT rabbits were harvested after euthanasia, homogenized in lysis buffer ((50 mM HEPES (pH 7.4), 150 mM NaCl, 1 mM EDTA, 1% NP-40, 10% glycerol with protease inhibitors cocktail (Roche 11836145001)) and centrifuged for 10 minutes at 10,000

rpm, 4°C. The concentration of total protein was tested by using protein assay dye reagent (Bio-Rad, 500-0006), and then, 50mg protein was resuspended in 6×SDS sample buffer and denatured at 42°C for 10 minutes. Protein samples were resolved by SDS-PAGE and transferred to PVDF membranes, which then were blocked at room temperature for 1 hour with 5% (w/v) skim milk powder in TBST (10 mM Tris (pH 8.0), 150 mM NaCl, 0.05% Tween 20). The blots were incubated with primary antibodies (596, 1: 5000 in TBST with 10% fetal bovine serum (FBS), from J. Riordan, University of North Carolina at Chapel Hill) at room temperature for 1 hour. The blots were then washed four times with TBST and incubated with horseradish peroxidase-conjugated secondary antibodies (1:5000, Abcam) in TBST with 10% FBS for 1 hour, followed by five washes with TBST. The reactive bands were visualized by incubation with enhanced chemiluminescence substrates (PerkinElmer Products) and exposure to X-ray film (Eastman Kodak Co). CFBE-o41 WT-CFTR cell lysate was used as the positive control.

### ***Immunofluorescence***

Lung lobes of CF and WT rabbits after euthanasia were perfused with 4% neutral paraformaldehyde (in 1×PBS, pH7.2) at a constant hydrostatic pressure and fixed in 4% neutral paraformaldehyde for 24 hours. Tissues were then cut into 0.5cm-thick pieces and gradually dehydrated in 5%, 20%, 30% sucrose solutions. Next, tissues were sectioned into 10µm thickness slices using a Cryotome. The tissues were then washed three times with buffer A (0.5% BSA and 0.15% glycine at pH 7.4 in phosphate-buffered saline). After blocking with purified goat serum, the sections were incubated with the appropriate primary antibodies (anti-CFTR 596, gift from University of North Carolina, <http://cftrantibodies.web.unc.edu/>, 1:300) for 1 hour followed by three washes in buffer A and subsequent incubation with fluorescein rhodamine -labeled secondary antibodies (1:300, Molecular Probes) for another hour. After washing with buffer A, the section was incubated with diluted DAPI solution for 5 minutes at room temperature, followed by

mounting with an anti-fade mounting media and imaged by confocal microscopy.

### ***Short-circuit recorded by Ussing chamber***

Tracheal preparations were prepared as 4 cm long sections of CF and WT rabbits that were excised and immediately placed into Ringer's Buffer (120mM NaCl, 25mM NaHCO<sub>3</sub>, 3.3mM KH<sub>2</sub>PO<sub>4</sub>, 0.8 mM K<sub>2</sub>HPO<sub>4</sub>, 1.2mM MgCl<sub>2</sub>, 1.2mM CaCl<sub>2</sub>, and 10mM glucose.) with 10 μM indomethacin, that was continuously gassed with 95% O<sub>2</sub> and 5% CO<sub>2</sub> for 10 minutes. After incubation, the trachea was placed under a dissection microscope and connective tissues were removed. A longitudinal cut was made along the trachea, exposing the mucosal side. The tracheal epithelium was carefully placed on a slider with an exposed surface area of 0.20 cm<sup>2</sup>. Both sides of the epithelium were perfused with equal amounts of Ringers' Buffer at 37°C. Both sides of the chamber were gassed with 95% O<sub>2</sub> and 5% CO<sub>2</sub>, providing gas lift circulation. Each sample was equilibrated under voltage clamp (short circuit, I<sub>sc</sub>) conditions for 20 minutes. Once incubation period was completed and a basal I<sub>sc</sub> was achieved, amiloride was added to the apical side of the chamber to a final concentration of 10<sup>-5</sup> M. Once a new steady-state was reached, forskolin was added to the basal side of the chamber, at a final concentration of 10<sup>-5</sup> M. Once a new steady steady-state was achieved, GlyH101 was added to the apical side of the chamber to a final concentration of 10 μM. Once a new steady-state was achieved, bumetanide was added to the basal side of the chamber to a final concentration of 10 μM. After a new steady-state was achieved, the tissue was allowed to re-equilibrate for 20 minutes and the experiment was completed. The Ussing chamber was an EM-CSYS-8 from Physiological Instruments.

### ***General histology staining***

Tissues were fixed in 10% neutral formaldehyde solution in PBS (pH7.2) for ~ 24 hours, embedded into paraffin blocks, and cut in to 10 μm sections.

For Hematoxylin and eosin (H&E) staining, after deparaffinization, sections were stained

in Mayer's hematoxylin solution for 8 minutes, and eosin-phloxine solution for 30 seconds to 1 minute. Sections were rinsed by running tap water between the two steps. After dehydration, sections were mounted with xylene based mounting medium.

For PAS staining, deparaffinized tissue sections were oxidized in 0.5% periodic acid solution for 5 minutes, stained with Schiff reagent for about 15 minutes, and washed in running water for about 5 minutes. After counterstaining in Mayer's hematoxylin for 1 minute, sections were washed in running water for 5 minutes. After dehydration, sections were mounted with xylene based mounting medium.

For Alcian blue staining, deparaffinized tissue sections were stained with Alcian blue for 15 minutes and then stained with Schiff's reagent for 10 minutes. After staining nuclei with haematoxylin, sections were mounted.

Collagen staining was achieved by using Gomori's trichrome stain kit (87020, Thermo): deparaffinized sections were placed in 40ml of Bouin's Fluid in a plastic coplin jar with a lid applied loosely and incubated at 56°C in a water bath for 1 hour. Sections were rinsed in running tap water for 5 minutes until the yellow color was removed. Sections were placed in Working Weigert's iron hematoxylin (solution A: B=1:1) and stained for 10 minutes. Sections were rinsed in running tap water for 10 minutes, stained in trichrome stain for 15 minutes, and then individual sections placed in 1% acetic acid solution for 1 minute and rinsed in deionized water for 30 seconds. Sections were mounted after dehydration.

### ***Bronchoalveolar lavage (BAL) fluid collection***

Rabbits were mounted on an operating table with ventral sides up after euthanasia. Neck and chest skin were shaved and disinfected with 70% alcohol. A 2cm longitudinal incision was made at the neck to expose the trachea, and a 15cm piece of suture thread was placed underneath the trachea. A 3cm PE tubing (4mm) on a three-way connector was inserted ~ 2.5 cm into the

trachea directed towards the lung. The tubing was secured in the trachea by tying with a suture. A syringe loaded with sterile PBS was attached to one side of the three-way connector for lavage. Lung was lavaged three times with 2 ml, 2 ml and 1 ml of sterile PBS and using a new syringe each time.

### ***BAL bacterial plates***

300  $\mu$ l fresh BAL was deposited on typical soy agar (TSA, BD 236950), Columbia ANA SB (BD 221928), Columbia CNA (BD 221352) and Chocolate II (BD 04082), and PSA (BD 292710) plates and cultured for 48 hours at 37 °C.

### ***BAL cytology***

To perform the total WBC cell counts in BAL fluid, 10  $\mu$ l BAL was loaded into a hemocytometer. Four corner squares of the hemocytometer were counted, and WBC cell count were calculated using the formula below:

$$\text{Total WBC cells/ml} = \text{Total WBC cell count in 4 squares} \times 2500$$

For quantification of neutrophils, 150  $\mu$ l BAL sample were loaded onto Cytospin slides (StatSpin and Iris, Chatsworth, CA, USA). Samples were cytocentrifuged at 1,000 rpm for 2 min. The cells deposited on the slide were air-dried and stained with Wright's stain (Sigma- Aldrich). In each case, more than 200 total cells were counted, and the percentage of neutrophils was calculated as the ratio of total #neutrophils/total counted cells.

### ***16S RNA sequencing***

The V4 region of 16S rRNA gene was amplified by PCR, where primers contained a unique barcode to distinguish specimens. The PCR amplicons were checked by agarose gel electrophoresis to ensure the product base pair length were as predicted and no non-specific amplification bands were present. Then PCR amplicons underwent high throughput sequencing using HiSeq 2500 rapid-run mode, which generated 250 bp paired-end reads.

In data analysis, we first removed adapters, PCR primers and low quality bases from each read. The data quality was identified using Fastqc software (<http://www.bioinformatics.babraham.ac.uk/projects/fastqc/>), and the low quality bases were removed by USEARCH tool ([www.drive5.com/usearch](http://www.drive5.com/usearch)). Because the total read length (250nt ´ 2) is longer than the PCR amplicon, the mate read pairs (ie, forward- and reverse-read) overlapped, and the USEARCH tool was used to identify the overlap region and merge the mate pairs. Second, the taxonomy assignments based on sequence alignments were computationally resolved using QIIME software ([www.qiime.org](http://www.qiime.org)). This analysis involves constructing Operational Taxonomic Units (OTUs) based on sequence similarity within the reads, picking a representative sequence from each OTU. We employed a hybrid approach: firstly, sequences were assigned to operational taxonomic units (OTUs) and clustered into phylotypes according to their similarity to previously annotated sequences in reference databases; secondly, the unmapped reads were used to construct OTUs by clustering sequences de novo, purely based on their similarity.

## **Results**

### ***CFTR functional expression in the GI tract, growth curves, and survival***

In rabbits, CFTR is widely expressed in the GI tract, including the jejunum and colon. The loss of CFTR in the GI tract results in failure to gain weight normally in CF subjects and in a small percentage of CF newborns, it can cause death due to meconium ileus [178-181].

The impact of the loss of CFTR function on the growth kinetics of CF vs. WT rabbits was assessed. At birth, CF rabbit kits had no significant differences in body weight or appearance compared to WT littermates (Figure 9F). CF kits failed to gain weight at the same rate as their WT counterparts after one month of age, a feature typical of CF children (Figure 9A, 9F). Administration of a laxative, Golytely, and a liquid supplement (Bio-Serv, cat. no. F1147SP) significantly improved the weight gain of CF rabbits. However, they did not approach the growth

rate of the WT controls (Figure 9F).

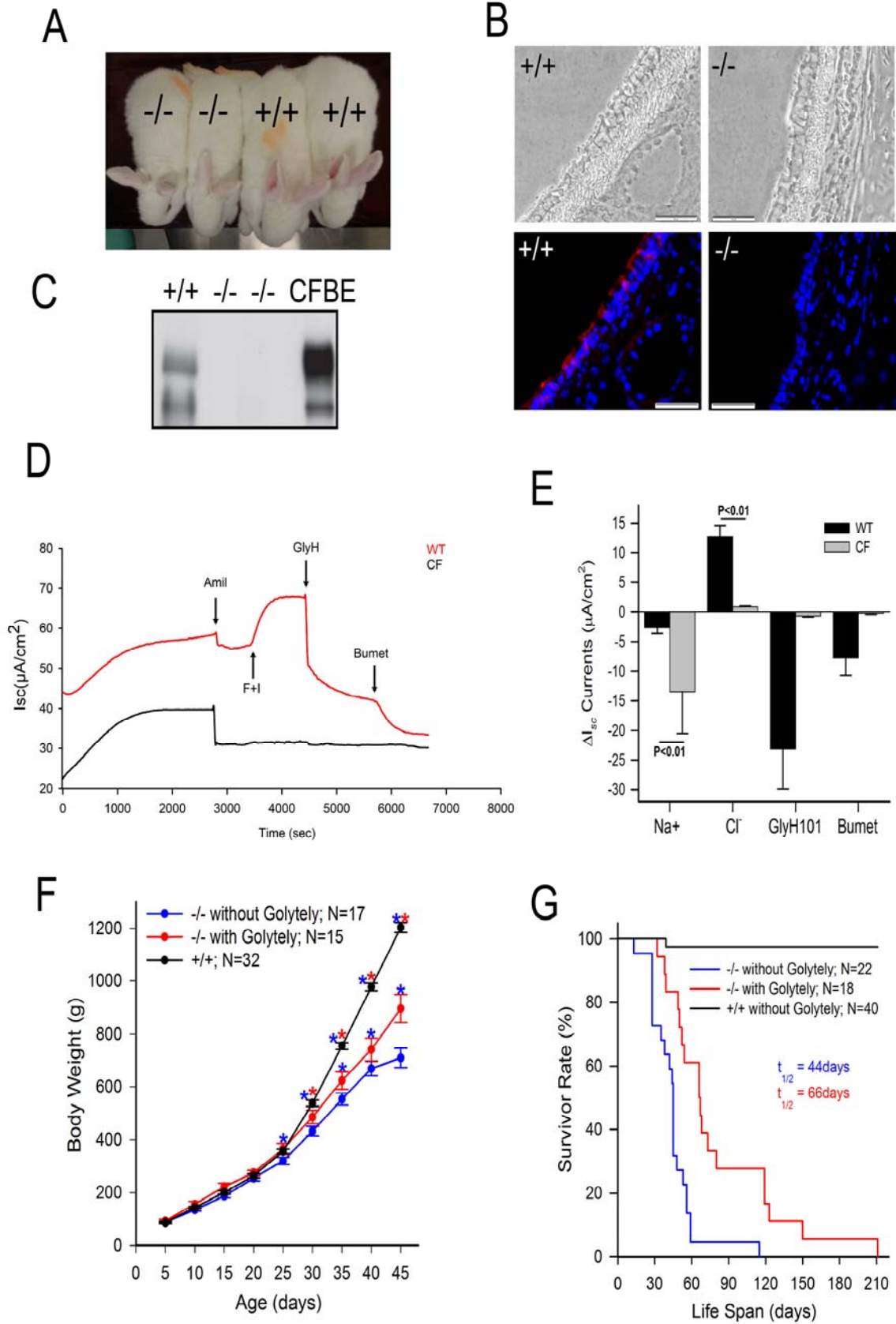


**Figure 9. Characterization of CF respiratory tract expression and function.** **A.** Overall appearance of WT (+/+) and a CF $\Delta$ 1 (-/-) rabbit at 44 days of age, illustrating the smaller size of CF rabbits as compared to WT littermates. **B.** Immunostaining of CFTR in tracheas from a WT and a CF rabbit, representative micrographs for differential interference contrast (upper panels) and immunofluorescence (lower panel). Scale bar 50  $\mu$ m **C.** CFTR western blots for normal human CFBE cultures alongside tissue lysates from CF and WT rabbit tracheas. **D.** A representative trace of a Ussing Chamber experiment of freshly excised rabbit trachea for a 1 WT rabbit and 1 CF rabbit **E.** Freshly excised rabbit tracheal short circuit currents (Isc) measurements in Ussing chambers. Isc changes in response to amiloride ( $10^{-4}$  M, apical), forskolin/Ibmx ( $10^{-4}$  and  $10^{-5}$  M, basolateral, respectively), GlyH101 (10  $\mu$ M, apical), and bumetanide ( $10^{-4}$  M, basolateral) are shown. N = 3 WT and 3 CF rabbits \*p < 0.05 different vs. WT. **F.** Body weight with age for WT rabbits (black), untreated CF rabbits without treatment (blue), and CF rabbits treated with Golytely starting at 2 weeks of age (red). \*p < 0.05 vs. untreated CF. **G.** Survival for WT and heterozygous rabbits (black, n=190), CF rabbits on Golytely (blue, n=23, and CF rabbits on Golytely, BioServe, and abdominal palpation-directed GI therapy (orange, n=38).

New Zealand White rabbits have a lifespan (7-10 years) that is comparable to both pigs and ferrets [182]. Survival curves showed that CF rabbits on a standard laboratory diet had a median age of survival, *i.e.*,  $t_{1/2}$ , of 44 days, significantly lower than their WT littermates ( $P < 0.01$ ; Figure 1G). The median survival of CF rabbits was significantly increased to  $t_{1/2}$  66 days when Golytely and a liquid diet were administered ( $P < 0.01$ ). It was possible to detect intestinal stasis/obstruction in pre-weaning CF rabbits (2 weeks) by routine abdominal palpation, and a protocol was developed to administer a “cocktail” of mucokinetic agents if intestinal masses were detected. This cocktail was effective ~ 70% of the time to eliminate palpable masses and restore weight gain. Rabbits treated with this regimen lived on average > 80 d (Figure 9D), significantly exceeding the lifespan of large animal CF models [103, 118, 183]

#### ***CFTR expression and function in rabbit lungs: loss of function in CF rabbits***

CFTR protein expression was next examined in the tracheas from CF vs WT rabbits. Like human bronchial epithelia (HBE), robust CFTR band B and C expression were observed in WT rabbits (Figure 9C). In contrast, western blot analysis failed to detect CFTR protein in the tracheas of CF rabbits. Immunofluorescence was also used to detect rabbit CFTR using the CFTR-596 antibody [184]. CFTR was localized to the apical membrane of WT rabbit tracheal epithelial cells,

whereas no tracheal epithelial CFTR expression was detected in CF rabbits (Figure 9B).

For bioelectric characterization of CFTR lower airway function, Ussing chambers were employed to measure short-circuit currents ( $I_{sc}$ ) across CF and non-CF tracheas (Figure 9D, 9E). Addition of forskolin and isobutylmethylxanthine (IBMX) to stimulate CFTR produced an increase in  $I_{sc}$  in the WT but not CF rabbits. Similarly, apical addition of the CFTR inhibitor, GlyH-101, decreased  $I_{sc}$  in WT but not CF rabbits. Finally, basolateral addition of bumetanide, an inhibitor of the  $\text{Na}^+\text{-K}^+\text{-2Cl}^-$  cotransporter, decreased  $I_{sc}$  in the WT tracheas but not CF tracheas. These results established the functional loss of CFTR-mediated anion secretion in the CF rabbit trachea.

As noted above, amiloride is a blocker of epithelial  $\text{Na}^+$  channel (ENaC) mediated  $\text{Na}^+$  absorption. As shown in Figure 9E, the amiloride-sensitive current was greater in CF than WT rabbits, consistent with accelerated  $\text{Na}^+$  absorption. However, given the interactions between  $\text{Na}^+$  and  $\text{Cl}^-$  conductance's in determining the magnitude of amiloride responses, isotope fluxes are required to confirm whether  $\text{Na}^+$  absorption is absolutely increased in CF rabbit tracheas [185, 186].

### ***Structural abnormalities in CF rabbit respiratory systems***

Like CF mice and pigs [103, 187-189], CF rabbit tracheas lacked the concentric ring pattern characteristic of their age matched WT counterparts (Figure 10A). With Alcian blue staining, the WT trachea showed complete cartilage ring formation with regular sizes and shapes (Figure 10B). In contrast, the CF tracheas exhibited irregular sizes and shapes, irregular cartilage rings, and thin bands of smooth muscle and fused cartilage (Figure 10B).

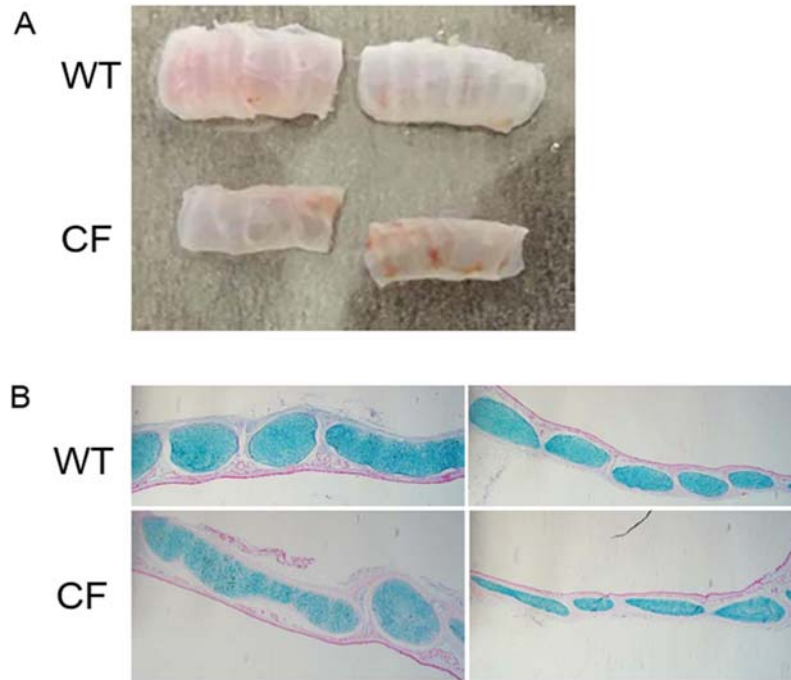
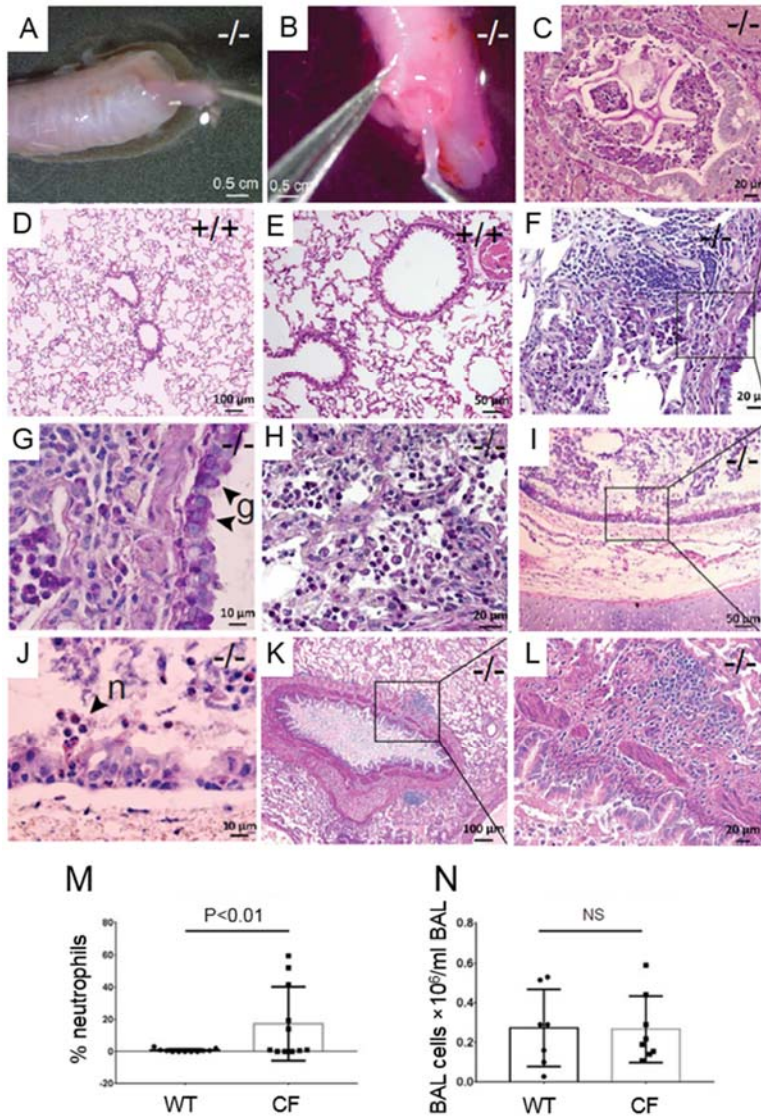


**Figure 10. Malformation of tracheal cartilaginous rings in CF rabbits.** **A.** Gross images of the tracheas from WT and CF rabbits. The tracheas from CF rabbits do not exhibit concentric and equally spaced cartilaginous rings as observed in WT rabbits. **B.** Representative micrographs of tracheal longitudinal sections from two WT and two CF rabbits stained with Alcian Blue, illustrating the aberrant shape and organization of cartilaginous rings in CF specimens.

### ***CF rabbit lung disease: mucus accumulation***

A major phenotype in CF subjects is defective airways mucociliary clearance [190, 191]. There is debate as to whether CF lung disease is initiated by large airway SMG dysfunction or defects in superficial epithelial mucus hydrating functions of small airways [105, 106, 183, 192-194]. The rabbit is an ideal species to study this issue because it lacks SMGs and like humans, but unlike rodents, expresses CFTR throughout distal (small) airway epithelia.

We visually observed the accumulation of mucus (*i.e.*, mucus plugs) in the airways of young (~ 40 d) CF rabbits (6 out of 30 examined, 20%). Mucus plugs were discovered in the trachea (Figure 11A), bronchi (Figure 11B), and in the bronchioles of CF rabbits (Figure 11C), but none in airways of the WT animals (Figure 11D, 11E).



Consistent with the importance of the superficial epithelium in rabbit lung pathophysiology, histologic staining revealed metaplastic/hyperplastic and distended goblet cells in the airways of CF as compared to WT rabbits (Figure 11F, 11G). In addition to mucus accumulation, inflammatory responses, including large numbers of neutrophils (Figure 11H-J) and macrophages in the lumen in parallel with submucosal bronchus-associated lymphoid tissue (BALT, Figure 11K, 11L) were observed in CF but not WT rabbits. Like neonatal human bronchoalveolar lavage (BAL) data [195, 196], the neutrophil percentage but not total cell number was significantly higher in CF vs. WT rabbit BAL (Figure 11M, 11N). Collectively, these data

mimic those of neonatal/young CF children who have increased airway mucus and inflammation [195, 197].

***CF rabbit lung disease: spontaneous bacterial infection***

To quantitate the incidence and identify the type of bacteria found in rabbit lungs, CF and WT rabbits were euthanized (median age 43 d) and BAL harvested. Culture of some CF BAL on TSA, ANA, CNA and Chocolate agar plates produced colony growth of anaerobes, facultative aerobic bacteria, gram-positive cocci, and gram-negative bacteria (Figure 12A). Overall, 13 out of

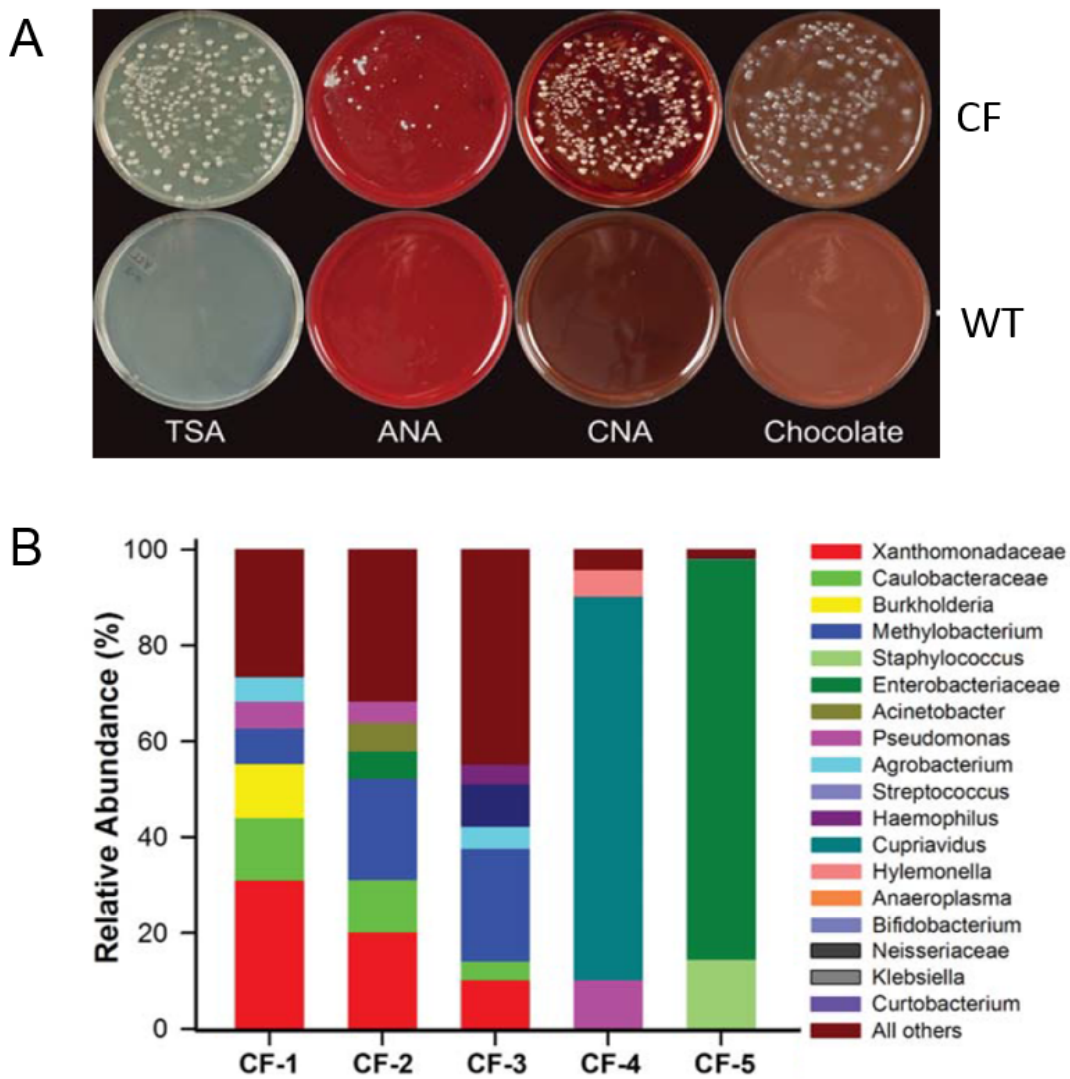


**Figure 12. Characterization of bacteria in bronchoalveolar lavage (BAL) from CF vs. WT rabbits. A.** CF vs WT BAL cultured on TSA, ANA, CNA and Chocolate plates. The plates were incubated in 37 °C for 48 hrs. **B.** 16S rRNA sequence analysis of bacteria species in BALF from five CF rabbits.

66 (19%) CF rabbits tested had positive BAL cultures for bacteria. None of the WT BALs (n=39) produced positive colonies on any plate (Figure 12A). 16S r RNA gene sequence analysis of five infected CF rabbits revealed polymicrobial species, including *Streptococcus*, *Micrococcaceae*, *Enterobacteriaceae*, *Staphylococcus*, and *Stenotrophomonas* (Figure 12B).

*Pseudomonas aeruginosa* was cultured (Figure 13A) in two CF rabbits who became moribund and were sacrificed at > 60 days of age (64 and 141 days, respectively). Grossly, the

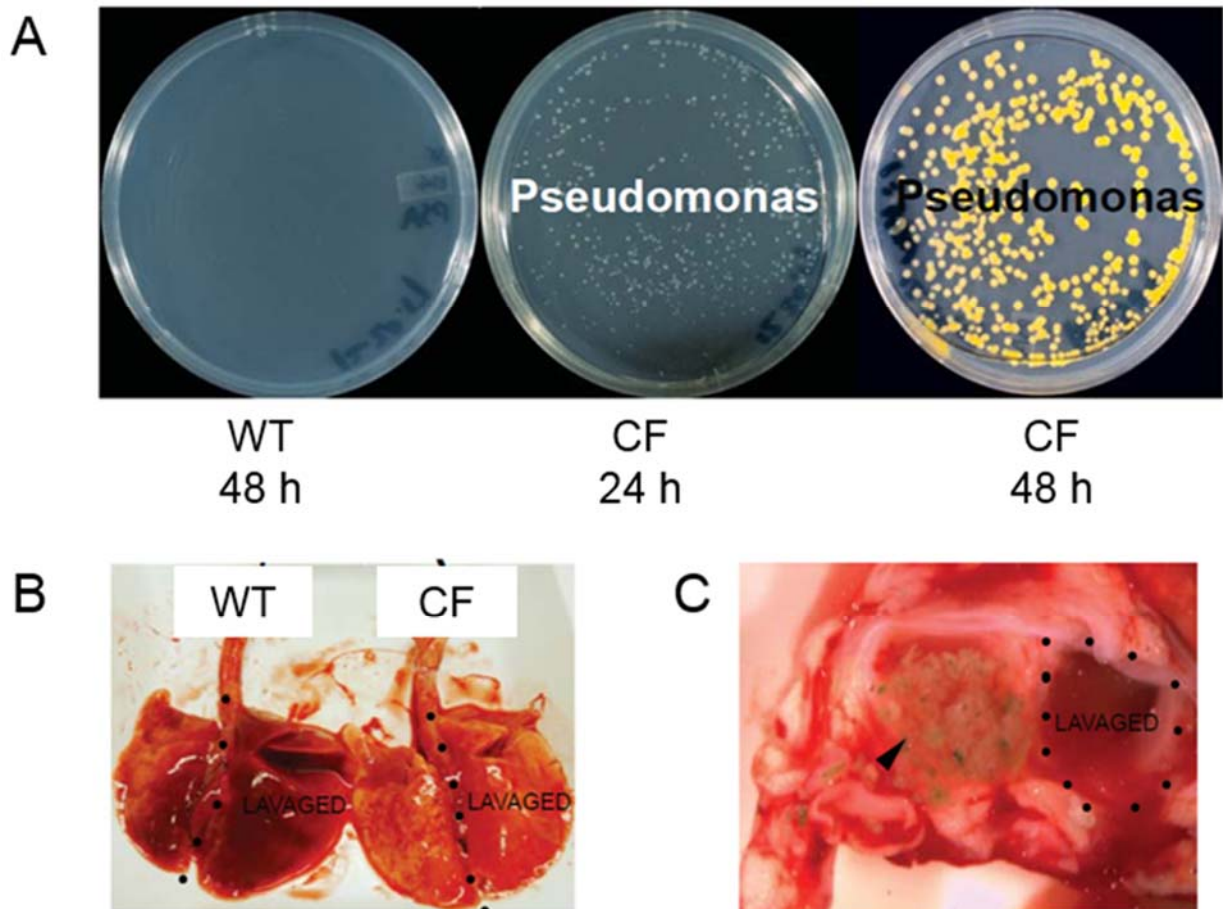


**Figure 13. Characterization of bacterial infection in bronchoalveolar lavage (BAL) from a moribund CF rabbit and WT age-matched control.** **A.** BALs were plated on *Pseudomonas aeruginosa* identification selective agar (TSA) and allowed to grow for 48 hours. Growth and progressive pigment development indicated the presence of *P. aeruginosa* in the CF specimen. **B.** Gross appearance of lungs from a wild-type and CF rabbit with *P. aeruginosa* infection. Note the mottled and inflated appearance of the left lobe in CF rabbit as compared to WT control. In each lung, the right lobes were subjected to BAL. **C.** The un-lavaged left main stem bronchus contained intraluminal mucus with visible black fibers and green dots, suggestive of bacterial macrocolonies and/or aspirated material.

lungs of one *Pseudomonas aeruginosa*-infected female CF rabbit exhibited a pale color with mottled discoloration, whereas the lungs of its WT littermate had a normal healthy appearance (Figure 13B). The left lobes of this rabbit were not lavaged and revealed that the left main stem bronchus was filled with mucus containing *Pseudomonas* macrocolonies associated with aspirated food (Figure 13C).

## **Discussion**

The rabbit was selected as a CF model because it provides fidelity of CFTR expression in the lung with respect to humans, exhibits high CFTR homology to human CFTR, and exhibits sensitivity to potentiators developed for CF pharmacotherapy. Important other features include the well-known breeding performance of rabbits, early weaning (~2-months of age), a size intermediate between current models, and relatively inexpensive housing costs.

The current CRISPR-derived indel genetic modifications of rabbit CFTR offer practical model for studies of CF pathogenesis and therapy. One practical feature of the rabbit is that female CF rabbits are fertile, making the generation of adequate rabbit numbers feasible. A second practical feature is that untreated CF rabbits do not exhibit the perinatal meconium ileus and mortality observed in the mouse and large animal models with a median survival of 44 days. The average lifespan could be extended to > 80 days with addition of a simple oral osmotic laxative/liquid diet and physical examination-based pharmacologic interventions.

There has been debate about the relative importance of large airway submucosal glands (SMG) vs small airways (no SMG) in the initiation of CF lung disease. In human CF, the first detectable abnormalities in lung pathology, radiology, and pulmonary function appear to be in the small airways [198-201]. However, these airways are more difficult to study in humans because of their protected/distal nature. The rabbit lung exhibits an architecture that resembles human small airways, including the absence of SMG, with a substantial club cell population [202]. Importantly,

unlike mice, the rabbit expresses CFTR like humans throughout distal airway regions.

Studies of human CF infant/children on a timed, *i.e.*, yearly basis, have emerged from the AREST CF cohort [203, 204]. AREST CF data have revealed that early CF lung disease is heterogeneous within the lung with a relatively small fraction of CF neonates/young children exhibiting bacterial infection by 3 years of age. Indeed, a muco-inflammatory environment is the first detectable event in the human CF lung, followed by infection by anaerobes and subsequently the classical CF pathogens, including *Pseudomonas* [203]. Similar timed protocols likely can be performed in future studies of CF rabbits but not in this early observational study focused on improving survival. However, we did identify visible mucus in the airways of CF rabbits and histological sections in ~ 11% of the CF rabbits by ~ 40 days that was accompanied by an increase in BAL neutrophil numbers/percentages. This visual analysis likely underestimated the mucus content in the lungs, as evidence from the AREST CF study suggests that most mucus from young CF subjects is manifest as small mucus plaques/plugs harvested as ~ 10-100  $\mu\text{m}$  “flakes” by BAL [205].

A spectrum of culture technologies designed to capture anaerobic, microaerophilic, and aerobic bacteria were employed to characterize lower airway bacterial infection in this study. An ~ 19% incidence of bacterial infection was noted in CF rabbits. Importantly, these infections were polymicrobial and dominated by anaerobic/microaerophilic bacteria. This polymicrobial infection and incidence rate mimicked data from the human AREST cohort [203]. Notably, the only two incidences of *Pseudomonas aeruginosa* infection occurred in older animals, typical of CF children. It should be noted that the CF rabbits were housed in a SPF facility that reduced/eliminated the possibility of intercurrent viral infections. In contrast, the AREST CF children had experienced multiple lower respiratory tract viral infections prior to/during the observational AREST study [206]. Thus, the next steps to test the relevance of CF rabbits to early human CF lung disease are

to raise rabbits in non-SPF environments and/or expose them to intermittent lower airway viral infections.

With respect to lower airways pathogenesis, the bioelectric properties of both the upper and lower airways in the CF rabbit mimic the typical bioelectric properties of human CF subjects. Namely, there was a virtual absence of forskolin-mediated anion secretion. Further, there was evidence for persistent and/or indeed raised sodium absorption (amiloride-sensitive PD/Isc) in both regions. As noted, ion fluxes will be required to confirm this notion. Regardless, the absence of anion secretion, coupled with persistent or, indeed, raised sodium transport, is predicted to dehydrate the airway surface environment, causing mucus hyperconcentration, mucus adhesion, and subsequent inflammation/bacterial infection [203, 205]. Importantly, the findings in the rabbit suggest the CF pathologic cascade can be mediated exclusively by the small airways epithelium in the absence of SMG defects.

### **Conclusion and Future Directions**

In summary, this study elucidated a molecular mechanism that is involved in F508del degradation and introduced a new animal model that mimicked human CF.

We found additional proteins that are involved in F508del degradation, and possible targets for therapeutic intervention. The E2 conjugating enzyme UBE 2L6, and its' interacting E3 ligase, RNF19B, both mediate the proteasomal degradation of F508del. Also, our data demonstrates that VX-809, an already established processing drug treatment, operates to enhance F508del function at the plasma membrane when UBE 2L6 and RNF19B are also silenced. Therefore, modulation of UBE 2L6/RNF19B mediated degradation of F508del offers a promising area for therapeutic intervention.

This study also introduces the CF rabbit model to the CF research community as an intermediate size model that is relevant to human CF pathogenesis and therapy. It manifests both

airway and GI phenotypes that are common to humans which are relatively easily measured for studies of CF pathogenesis. The CF rabbits also exhibit straightforward readouts of CFTR function for pharmacotherapy/genetic therapy, including: 1) lower airways bioelectric, infection, mucus plugging, and inflammation; and 2) abnormal weight loss and survival. Future improvements in animal husbandry may make the rabbit model even more useful, including gut-corrected rabbits and G551D rabbits that may be maintained on potentiators.

Interestingly, UBE 2L6 is highly expressed in human lung tissue, compared to other organs [207]. Therefore, future studies will look into using the CRISPR/Cas9 system to knock in F508del mutation into rabbits and examine the expression level of UBE 2L6 in F508del rabbits compared to WT rabbits. It will be interesting to see if F508del knock-in rabbits have a higher expression of UBE 2L6 in the lungs compared to WT rabbits. The higher expression may result in a swifter degradation of F508del protein, contributing to a severe lung phenotype that may be comparable to human CF. This same tactic can be used to investigate RNF19B expression levels in the lungs. Previous studies in mice tissue showed that several E3 ligases, including RNF19B, was upregulated by ER stress [208]. F508del that is retained in the ER activates the unfolded protein response, a form of ER stress [209], therefore RNF19B expression in the lungs may also be upregulated. Therefore, future studies in the rabbit model may try to highlight targeting the UPR in airway inflammation and target the UPR as a therapeutic strategy for CF related airway disease.

**APPENDIX**

**IACUC Approval Letter**



Institutional Animal Care  
And Use Committee  
87 East Canfield, Second Floor  
Detroit, Michigan 48201  
Phone: (313) 577-1629

---

**ANIMAL WELFARE ASSURANCE # D16-00198 (A3310-01)**

**TO:** Fei Sun  
Physiology

**FROM:** Institutional Animal Care and Use Committee

**DATE:** May 31, 2017

**SUBJECT:** Approval of Protocol 17-03-242

**TITLE:** Rabbit Model for Cystic Fibrosis

**Protocol Effective Period:** May 31, 2017 - May 30, 2020

Your animal research protocol has been approved by the Wayne State University Institutional Animal Care and Use Committee (IACUC).

Be advised that this protocol must be reviewed by the IACUC on an annual basis to remain active. Any changes (e.g. procedures, lab personnel, strains, additional numbers of animals) must be submitted as amendments and require prior approval by the IACUC. Any animal work on this research protocol beyond the expiration date will require the submission of a new IACUC protocol application for committee review and approval.

*The Guide for the Care and Use of Laboratory Animals* (the Guide, NRC 2011) is the primary reference used for standards of animal care at Wayne State University. The University has submitted an appropriate assurance statement to the Office for Laboratory Animal Welfare (OLAW) of the National Institutes of Health. The animal care program at Wayne State University is accredited by the Association for Assessment and Accreditation of Laboratory Animal Care International (AAALAC).

## REFERENCES

1. Pilewski, J.M. and R.A. Frizzell, *Role of CFTR in airway disease*. *Physiol Rev*, 1999. **79**(1 Suppl): p. S215-55.
2. Welsh, M.J. and B.W. Ramsey, *Research on cystic fibrosis: a journey from the Heart House*. *Am J Respir Crit Care Med*, 1998. **157**(4 Pt 2): p. S148-54.
3. Boucher, R.C., *An overview of the pathogenesis of cystic fibrosis lung disease*. *Advanced Drug Delivery Reviews*, 2002. **54**(11): p. 1359-1371.
4. Boucher, R.C., *Airway surface dehydration in cystic fibrosis: pathogenesis and therapy*. *Annu Rev Med*, 2007. **58**: p. 157-70.
5. Perez-Vilar, J. and R.C. Boucher, *Reevaluating gel-forming mucins' roles in cystic fibrosis lung disease*. *Free Radical Biology and Medicine*, 2004. **37**(10): p. 1564-1577.
6. Welsh, M.J. and A.E. Smith, *Molecular mechanisms of CFTR chloride channel dysfunction in cystic fibrosis*. *Cell*, 1993. **73**(7): p. 1251-1254.
7. Riordan, J.R., et al., *Identification of the cystic fibrosis gene: cloning and characterization of complementary DNA*. *Science*, 1989. **245**(4922): p. 1066-73.
8. Cyr, D.M., *Arrest of CFTR $\Delta$ F508 folding*. *Nat Struct Mol Biol*, 2005. **12**(1): p. 2-3.
9. Denning, G.M., et al., *Processing of mutant cystic fibrosis transmembrane conductance regulator is temperature-sensitive*. *Nature*, 1992. **358**(6389): p. 761-4.
10. Drumm, M.L., et al., *Chloride conductance expressed by delta F508 and other mutant CFTRs in *Xenopus* oocytes*. *Science*, 1991. **254**(5039): p. 1797-9.
11. Brown, C.R., et al., *Chemical chaperones correct the mutant phenotype of the delta F508 cystic fibrosis transmembrane conductance regulator protein*. *Cell Stress Chaperones*, 1996. **1**(2): p. 117-25.

12. Loo, M.A., et al., *Perturbation of Hsp90 interaction with nascent CFTR prevents its maturation and accelerates its degradation by the proteasome*. *Embo j*, 1998. **17**(23): p. 6879-87.
13. Meacham, G.C., et al., *The Hdj-2/Hsc70 chaperone pair facilitates early steps in CFTR biogenesis*. *Embo j*, 1999. **18**(6): p. 1492-505.
14. Yang, Y., et al., *The common variant of cystic fibrosis transmembrane conductance regulator is recognized by hsp70 and degraded in a pre-Golgi nonlysosomal compartment*. *Proc Natl Acad Sci U S A*, 1993. **90**(20): p. 9480-4.
15. Qu, B.H., E.H. Strickland, and P.J. Thomas, *Localization and suppression of a kinetic defect in cystic fibrosis transmembrane conductance regulator folding*. *J Biol Chem*, 1997. **272**(25): p. 15739-44.
16. Varga, K., et al., *Efficient intracellular processing of the endogenous cystic fibrosis transmembrane conductance regulator in epithelial cell lines*. *J Biol Chem*, 2004. **279**(21): p. 22578-84.
17. Ward, C.L. and R.R. Kopito, *Intracellular turnover of cystic fibrosis transmembrane conductance regulator. Inefficient processing and rapid degradation of wild-type and mutant proteins*. *J Biol Chem*, 1994. **269**(41): p. 25710-8.
18. Kreda, S.M., et al., *Characterization of wild-type and deltaF508 cystic fibrosis transmembrane regulator in human respiratory epithelia*. *Molecular biology of the cell*, 2005. **16**(5): p. 2154-2167.
19. Jensen, T.J., et al., *Multiple proteolytic systems, including the proteasome, contribute to CFTR processing*. *Cell*, 1995. **83**(1): p. 129-35.
20. Younger, J.M., et al., *A foldable CFTR{Delta}F508 biogenic intermediate accumulates upon inhibition of the Hsc70-CHIP E3 ubiquitin ligase*. *J Cell Biol*, 2004. **167**(6):1075-85.

21. Ward, C.L., S. Omura, and R.R. Kopito, *Degradation of CFTR by the ubiquitin-proteasome pathway*. Cell, 1995. **83**(1): p. 121-127.
22. Meacham, G.C., et al., *The Hsc70 co-chaperone CHIP targets immature CFTR for proteasomal degradation*. Nat Cell Biol, 2001. **3**(1): p. 100-5.
23. Vij, N., S. Fang, and P.L. Zeitlin, *Selective inhibition of endoplasmic reticulum-associated degradation rescues DeltaF508-cystic fibrosis transmembrane regulator and suppresses interleukin-8 levels: therapeutic implications*. J Biol Chem, 2006. **281**(25): p. 17369-78.
24. Younger, J.M., et al., *Sequential Quality-Control Checkpoints Triage Misfolded Cystic Fibrosis Transmembrane Conductance Regulator*. Cell, 2006. **126**(3): p. 571-582.
25. Carlson, E.J., D. Pitonzo, and W.R. Skach, *p97 functions as an auxiliary factor to facilitate TM domain extraction during CFTR ER-associated degradation*. Embo j, 2006. **25**(19): p. 4557-66.
26. Sun, F., et al., *Derlin-1 promotes the efficient degradation of the cystic fibrosis transmembrane conductance regulator (CFTR) and CFTR folding mutants*. J Biol Chem, 2006. **281**(48): p. 36856-63.
27. Welch, W.J., *Role of quality control pathways in human diseases involving protein misfolding*. Semin Cell Dev Biol, 2004. **15**(1): p. 31-8.
28. Rowe, S.M., S. Miller, and E.J. Sorscher, *Cystic fibrosis*. N Engl J Med, 2005. **352**(19): p. 1992-2001.
29. Patrick, A.E. and P.J. Thomas, *Development of CFTR Structure*. Front Pharmacol, 2012. **3**: p. 162.
30. Wang, W., et al., *Relative contribution of different transmembrane segments to the CFTR chloride channel pore*. Pflugers Arch, 2014. **466**(3): p. 477-90.

31. Chappe, V., et al., *Phosphorylation of CFTR by PKA promotes binding of the regulatory domain*. *Embo j*, 2005. **24**(15): p. 2730-40.
32. Naren, A.P., et al., *CFTR chloride channel regulation by an interdomain interaction*. *Science*, 1999. **286**(5439): p. 544-8.
33. Sheppard, D.N. and M.J. Welsh, *Structure and function of the CFTR chloride channel*. *Physiol Rev*, 1999. **79**(1 Suppl): p. S23-45.
34. Naren, A.P., et al., *Syntaxin 1A inhibits CFTR chloride channels by means of domain-specific protein-protein interactions*. *Proc Natl Acad Sci U S A*, 1998. **95**(18): p. 10972-7.
35. Gene, G.G., et al., *N-terminal CFTR missense variants severely affect the behavior of the CFTR chloride channel*. *Hum Mutat*, 2008. **29**(5): p. 738-49.
36. Caputo, A., et al., *Mutation-Specific Potency and Efficacy of Cystic Fibrosis Transmembrane Conductance Regulator Chloride Channel Potentiators*. *Journal of Pharmacology and Experimental Therapeutics*, 2009. **330**(3): p. 783.
37. Loo, T.W. and D.M. Clarke, *The Transmission Interfaces Contribute Asymmetrically to the Assembly and Activity of Human P-glycoprotein*. *J Biol Chem*, 2015. **290**(27): p. 16954-63.
38. Cremonesi, L., et al., *Four new mutations of the CFTR gene (541delC, R347H, R352Q, E585X) detected by DGGE analysis in Italian CF patients, associated with different clinical phenotypes*. *Hum Mutat*, 1992. **1**(4): p. 314-9.
39. Billet, A., et al., *CFTR: effect of ICL2 and ICL4 amino acids in close spatial proximity on the current properties of the channel*. *J Cyst Fibros*, 2013. **12**(6): p. 737-45.
40. Ghanem, N., et al., *Identification of eight mutations and three sequence variations in the cystic fibrosis transmembrane conductance regulator (CFTR) gene*. *Genomics*, 1994. **21**(2): p. 434-6.

41. Seibert, F.S., et al., *Cytoplasmic loop three of cystic fibrosis transmembrane conductance regulator contributes to regulation of chloride channel activity*. J Biol Chem, 1996. **271**(44): p. 27493-9.
42. Vankeerberghen, A., et al., *Characterization of mutations located in exon 18 of the CFTR gene*. FEBS Lett, 1998. **437**(1-2): p. 1-4.
43. Hammerle, M.M., A.A. Aleksandrov, and J.R. Riordan, *Disease-associated mutations in the extracytoplasmic loops of cystic fibrosis transmembrane conductance regulator do not impede biosynthetic processing but impair chloride channel stability*. J Biol Chem, 2001. **276**(18): p. 14848-54.
44. Kristidis, P., et al., *Genetic determination of exocrine pancreatic function in cystic fibrosis*. American journal of human genetics, 1992. **50**(6): p. 1178-1184.
45. Infield, D.T., et al., *Positioning of extracellular loop 1 affects pore gating of the cystic fibrosis transmembrane conductance regulator*. Am J Physiol Lung Cell Mol Physiol, 2016. **310**(5): p. L403-14.
46. Wang, Y.-J., X.-J. Di, and T.-W. Mu, *Using pharmacological chaperones to restore proteostasis*. Pharmacological Research, 2014. **83**(0): p. 3-9.
47. Zang, X., et al., *Comparison of Ambient and Atmospheric Pressure Ion Sources for Cystic Fibrosis Exhaled Breath Condensate Ion Mobility-Mass Spectrometry Metabolomics*. J Am Soc Mass Spectrom, 2017. **28**(8): p. 1489-1496.
48. Therien, A.G., F.E. Grant, and C.M. Deber, *Interhelical hydrogen bonds in the CFTR membrane domain*. Nat Struct Biol, 2001. **8**(7): p. 597-601.
49. Partridge, A.W., R.A. Melnyk, and C.M. Deber, *Polar residues in membrane domains of proteins: molecular basis for helix-helix association in a mutant CFTR transmembrane segment*. Biochemistry, 2002. **41**(11): p. 3647-53.

50. Belmonte, L. and O. Moran, *On the interactions between nucleotide binding domains and membrane spanning domains in cystic fibrosis transmembrane regulator: A molecular dynamic study*. Biochimie, 2015. **111**: p. 19-29.
51. Schreiber, R., et al., *The first-nucleotide binding domain of the cystic-fibrosis transmembrane conductance regulator is important for inhibition of the epithelial Na<sup>+</sup> channel*. Proc Natl Acad Sci U S A, 1999. **96**(9): p. 5310-5.
52. Yuan, Y.R., et al., *The crystal structure of the MJ0796 ATP-binding cassette. Implications for the structural consequences of ATP hydrolysis in the active site of an ABC transporter*. J Biol Chem, 2001. **276**(34): p. 32313-21.
53. Xiong, X., et al., *Structural cues involved in endoplasmic reticulum degradation of G85E and G91R mutant cystic fibrosis transmembrane conductance regulator*. J Clin Invest, 1997. **100**(5): p. 1079-88.
54. Vernon, R.M., et al., *Stabilization of a nucleotide-binding domain of the cystic fibrosis transmembrane conductance regulator yields insight into disease-causing mutations*. J Biol Chem, 2017. **292**(34): p. 14147-14164.
55. Seibert, F.S., et al., *Influence of phosphorylation by protein kinase A on CFTR at the cell surface and endoplasmic reticulum*. Biochim Biophys Acta, 1999. **1461**(2): p. 275-83.
56. Aznarez, I., et al., *Characterization of disease-associated mutations affecting an exonic splicing enhancer and two cryptic splice sites in exon 13 of the cystic fibrosis transmembrane conductance regulator gene*. Hum Mol Genet, 2003. **12**(16): p. 2031-40.
57. Choi, J.Y., et al., *Aberrant CFTR-dependent HCO<sub>3</sub><sup>-</sup> transport in mutations associated with cystic fibrosis*. Nature, 2001. **410**(6824): p. 94-7.
58. Lavelle, G.M., et al., *Animal Models of Cystic Fibrosis Pathology: Phenotypic Parallels and Divergences*. Biomed Res Int, 2016. **2016**: p. 5258727.

59. Marunaka, Y., *The Mechanistic Links between Insulin and Cystic Fibrosis Transmembrane Conductance Regulator (CFTR) Cl(-) Channel*. Int J Mol Sci, 2017. **18**(8).
60. Veit, G., et al., *From CFTR biology toward combinatorial pharmacotherapy: expanded classification of cystic fibrosis mutations*. Molecular Biology of the Cell, 2016. **27**(3): p. 424-433.
61. Sosnay, P.R., et al., *Defining the disease liability of variants in the cystic fibrosis transmembrane conductance regulator gene*. Nat Genet, 2013. **45**(10): p. 1160-7.
62. Dupuis, A., et al., *Prevalence of meconium ileus marks the severity of mutations of the Cystic Fibrosis Transmembrane Conductance Regulator (CFTR) gene*. Genet Med, 2016. **18**(4): p. 333-40.
63. Zielenski, J., *Genotype and phenotype in cystic fibrosis*. Respiration, 2000. **67**(2):117-33.
64. Van Goor, F., et al., *Effect of ivacaftor on CFTR forms with missense mutations associated with defects in protein processing or function*. J Cyst Fibros, 2014. **13**(1): p. 29-36.
65. Ratjen, F., et al., *Efficacy and safety of lumacaftor and ivacaftor in patients aged 6-11 years with cystic fibrosis homozygous for F508del-CFTR: a randomised, placebo-controlled phase 3 trial*. Lancet Respir Med, 2017. **5**(7): p. 557-567.
66. Romisch, K., *Endoplasmic reticulum-associated degradation*. Annu Rev Cell Dev Biol, 2005. **21**: p. 435-56.
67. Ellgaard, L. and A. Helenius, *Quality control in the endoplasmic reticulum*. Nat Rev Mol Cell Biol, 2003. **4**(3): p. 181-91.
68. Brodsky, J.L. and A.A. McCracken, *ER protein quality control and proteasome-mediated protein degradation*. Semin Cell Dev Biol, 1999. **10**(5): p. 507-13.
69. Trombetta, E.S. and A.J. Parodi, *Quality control and protein folding in the secretory pathway*. Annu Rev Cell Dev Biol, 2003. **19**: p. 649-76.

70. Gething, M.J. and J. Sambrook, *Protein folding in the cell*. Nature, 1992. **355**(6355):33-45.
71. Helenius, A., T. Marquardt, and I. Braakman, *The endoplasmic reticulum as a protein-folding compartment*. Trends Cell Biol, 1992. **2**(8): p. 227-31.
72. Kopito, R.R., *ER Quality Control: The Cytoplasmic Connection*. Cell. **88**(4): p. 427-430.
73. Carvalho, P., V. Goder, and T.A. Rapoport, *Distinct ubiquitin-ligase complexes define convergent pathways for the degradation of ER proteins*. Cell, 2006. **126**(2): p. 361-73.
74. Denic, V., E.M. Quan, and J.S. Weissman, *A luminal surveillance complex that selects misfolded glycoproteins for ER-associated degradation*. Cell, 2006. **126**(2): p. 349-59.
75. Vashist, S. and D.T. Ng, *Misfolded proteins are sorted by a sequential checkpoint mechanism of ER quality control*. J Cell Biol, 2004. **165**(1): p. 41-52.
76. Madsen, L., et al., *New ATPase regulators—p97 goes to the PUB*. The International Journal of Biochemistry & Cell Biology, 2009. **41**(12): p. 2380-2388.
77. Wang, X., et al., *The viral E3 ubiquitin ligase mK3 uses the Derlin/p97 endoplasmic reticulum-associated degradation pathway to mediate down-regulation of major histocompatibility complex class I proteins*. J Biol Chem, 2006. **281**(13): p. 8636-44.
78. Sun, F., et al., *Chaperone displacement from mutant cystic fibrosis transmembrane conductance regulator restores its function in human airway epithelia*. Faseb j, 2008. **22**(9): p. 3255-63.
79. Wiertz, E.J., et al., *Sec61-mediated transfer of a membrane protein from the endoplasmic reticulum to the proteasome for destruction*. Nature, 1996. **384**(6608): p. 432-8.
80. Wiertz, E.J., et al., *The human cytomegalovirus US11 gene product dislocates MHC class I heavy chains from the endoplasmic reticulum to the cytosol*. Cell, 1996. **84**(5): p. 769-79.

81. Ye, Y., et al., *A membrane protein complex mediates retro-translocation from the ER lumen into the cytosol*. Nature, 2004. **429**(6994): p. 841-7.
82. Lilley, B.N. and H.L. Ploegh, *A membrane protein required for dislocation of misfolded proteins from the ER*. Nature, 2004. **429**(6994): p. 834-40.
83. Deshaies, R.J. and C.A. Joazeiro, *RING domain E3 ubiquitin ligases*. Annu Rev Biochem, 2009. **78**: p. 399-434.
84. Claessen, J.H.L., L. Kundrat, and H.L. Ploegh, *Protein quality control in the ER: balancing the ubiquitin checkbook*. Trends in cell biology, 2012. **22**(1): p. 22-32.
85. Bence, N.F., R.M. Sampat, and R.R. Kopito, *Impairment of the ubiquitin-proteasome system by protein aggregation*. Science, 2001. **292**(5521): p. 1552-5.
86. Kleiger, G. and T. Mayor, *Perilous journey: a tour of the ubiquitin-proteasome system*. Trends Cell Biol, 2014. **24**(6): p. 352-9.
87. Adams, J., *The proteasome: structure, function, and role in the cell*. Cancer Treat Rev, 2003. **29 Suppl 1**: p. 3-9.
88. Gong, B., et al., *The Ubiquitin-Proteasome System: Potential Therapeutic Targets for Alzheimer's Disease and Spinal Cord Injury*. Front Mol Neurosci, 2016. **9**: p. 4.
89. Song, L. and Z.Q. Luo, *Post-translational regulation of ubiquitin signaling*. J Cell Biol, 2019.
90. Li, W. and Y. Ye, *Polyubiquitin chains: functions, structures, and mechanisms*. Cell Mol Life Sci, 2008. **65**(15): p. 2397-406.
91. McClure, M.L., et al., *Trafficking and function of the cystic fibrosis transmembrane conductance regulator: a complex network of posttranslational modifications*. Am J Physiol Lung Cell Mol Physiol, 2016. **311**(4): p. L719-L733.

92. Michel, M.A., et al., *Assembly and specific recognition of k29- and k33-linked polyubiquitin*. Mol Cell, 2015. **58**(1): p. 95-109.
93. Xu, P., et al., *Quantitative proteomics reveals the function of unconventional ubiquitin chains in proteasomal degradation*. Cell, 2009. **137**(1): p. 133-45.
94. Brodsky, J.L., A. Merz, and T. Serio, *Organelle and proteome quality control mechanisms: how cells are able to keep calm and carry on*. Mol Biol Cell, 2014. **25**(6): p. 733-4.
95. Morito, D., et al., *Gp78 cooperates with RMA1 in endoplasmic reticulum-associated degradation of CFTRDeltaF508*. Mol Biol Cell, 2008. **19**(4): p. 1328-36.
96. Ballar, P., et al., *Differential regulation of CFTRDeltaF508 degradation by ubiquitin ligases gp78 and Hrd1*. The International Journal of Biochemistry & Cell Biology, 2010. **42**(1): p. 167-173.
97. Koeppen, K., et al., *Nedd4-2 does not regulate wt-CFTR in human airway epithelial cells*. Am J Physiol Lung Cell Mol Physiol, 2012. **303**(8): p. L720-7.
98. Caohuy, H., C. Jozwik, and H.B. Pollard, *Rescue of DeltaF508-CFTR by the SGK1/Nedd4-2 signaling pathway*. J Biol Chem, 2009. **284**(37): p. 25241-53.
99. El Khouri, E., et al., *RNF185 is a novel E3 ligase of endoplasmic reticulum-associated degradation (ERAD) that targets cystic fibrosis transmembrane conductance regulator (CFTR)*. J Biol Chem, 2013. **288**(43): p. 31177-91.
100. Ratjen, F., et al., *Cystic fibrosis*. Nat Rev Dis Primers, 2015. **1**: p. 15010.
101. Rosen, B.H., et al., *Animal and model systems for studying cystic fibrosis*. J Cyst Fibros, 2018. **17**(2s): p. S28-s34.
102. Kent, G., et al., *Lung disease in mice with cystic fibrosis*. J Clin Invest, 1997. **100**(12): p. 3060-9.

103. Fan, Z., et al., *A sheep model of cystic fibrosis generated by CRISPR/Cas9 disruption of the CFTR gene*. JCI Insight, 2018. **3**(19).
104. Tuggle, K.L., et al., *Characterization of defects in ion transport and tissue development in cystic fibrosis transmembrane conductance regulator (CFTR)-knockout rats*. PLoS One, 2014. **9**(3): p. e91253.
105. Ermund, A., et al., *The mucus bundles responsible for airway cleaning are retained in cystic fibrosis and by cholinergic stimulation*. Eur Respir J, 2018. **52**(2).
106. Stoltz, D.A., et al., *Cystic fibrosis pigs develop lung disease and exhibit defective bacterial eradication at birth*. Sci Transl Med, 2010. **2**(29): p. 29ra31.
107. Mall, M., et al., *Increased airway epithelial Na<sup>+</sup> absorption produces cystic fibrosis-like lung disease in mice*. Nat Med, 2004. **10**(5): p. 487-93.
108. Fisher, J.T., Y. Zhang, and J.F. Engelhardt, *Comparative biology of cystic fibrosis animal models*. Methods Mol Biol, 2011. **742**: p. 311-34.
109. Snouwaert, J.N., et al., *An animal model for cystic fibrosis made by gene targeting*. Science, 1992. **257**(5073): p. 1083-8.
110. Tarran, R., et al., *The CF salt controversy: in vivo observations and therapeutic approaches*. Mol Cell, 2001. **8**(1): p. 149-58.
111. Festini, F., et al., *Isolation measures for prevention of infection with respiratory pathogens in cystic fibrosis: a systematic review*. J Hosp Infect, 2006. **64**(1): p. 1-6.
112. Shah, V.S., et al., *Airway acidification initiates host defense abnormalities in cystic fibrosis mice*. Science, 2016. **351**(6272): p. 503-7.
113. Clarke, L.L., et al., *Relationship of a non-cystic fibrosis transmembrane conductance regulator-mediated chloride conductance to organ-level disease in Cfr(-/-) mice*. Proc Natl Acad Sci U S A, 1994. **91**(2): p. 479-83.

114. Gosselin, D., et al., *Impaired ability of Cftr knockout mice to control lung infection with Pseudomonas aeruginosa*. Am J Respir Crit Care Med, 1998. **157**(4 Pt 1): p. 1253-62.
115. Navis, A. and M. Bagnat, *Loss of cftr function leads to pancreatic destruction in larval zebrafish*. Dev Biol, 2015. **399**(2): p. 237-48.
116. Welsh, M.J., et al., *Development of a porcine model of cystic fibrosis*. Trans Am Clin Climatol Assoc, 2009. **120**: p. 149-62.
117. Rogers, C.S., et al., *Production of CFTR-null and CFTR-DeltaF508 heterozygous pigs by adeno-associated virus-mediated gene targeting and somatic cell nuclear transfer*. J Clin Invest, 2008. **118**(4): p. 1571-7.
118. Rogers, C.S., et al., *Disruption of the CFTR gene produces a model of cystic fibrosis in newborn pigs*. Science, 2008. **321**(5897): p. 1837-41.
119. Wine, J.J., *The development of lung disease in cystic fibrosis pigs*. Sci Transl Med, 2010. **2**(29): p. 29ps20.
120. Meyerholz, D.K., et al., *Pathology of Gastrointestinal Organs in a Porcine Model of Cystic Fibrosis*. The American Journal of Pathology, 2010. **176**(3): p. 1377-1389.
121. Stoltz, D.A., et al., *Intestinal CFTR expression alleviates meconium ileus in cystic fibrosis pigs*. J Clin Invest, 2013. **123**(6): p. 2685-93.
122. Olivier, A.K., K.N. Gibson-Corley, and D.K. Meyerholz, *Animal models of gastrointestinal and liver diseases. Animal models of cystic fibrosis: gastrointestinal, pancreatic, and hepatobiliary disease and pathophysiology*. Am J Physiol Gastrointest Liver Physiol, 2015. **308**(6): p. G459-71.
123. Wang, Y., et al., *Targeted proteasome inhibition by Velcade induces apoptosis in human mesothelioma and breast cancer cell lines*. Cancer Chemotherapy and Pharmacology, 2010. **66**(3): p. 455-466.

124. Sun, X., et al., *Lung phenotype of juvenile and adult cystic fibrosis transmembrane conductance regulator-knockout ferrets*. *Am J Respir Cell Mol Biol*, 2014. **50**(3): p. 502-12.
125. Sun, X., et al., *Disease phenotype of a ferret CFTR-knockout model of cystic fibrosis*. *The Journal of Clinical Investigation*, 2010. **120**(9): p. 3149-3160.
126. Sun, X., et al., *Gastrointestinal pathology in juvenile and adult CFTR-knockout ferrets*. *Am J Pathol*, 2014. **184**(5): p. 1309-22.
127. Keiser, N.W., et al., *Defective Innate Immunity and Hyperinflammation in Newborn Cystic Fibrosis Transmembrane Conductance Regulator–Knockout Ferret Lungs*. *American Journal of Respiratory Cell and Molecular Biology*, 2014. **52**(6): p. 683-694.
128. Abraham, W.M., *Modeling of asthma, COPD and cystic fibrosis in sheep*. *Pulm Pharmacol Ther*, 2008. **21**(5): p. 743-54.
129. Allen, J.E., et al., *Animal models of airway inflammation and airway smooth muscle remodelling in asthma*. *Pulm Pharmacol Ther*, 2009. **22**(5): p. 455-65.
130. Scholte, B.J., et al., *Cellular and animal models of cystic fibrosis, tools for drug discovery*. *Drug Discovery Today: Disease Models*, 2006. **3**(3): p. 251-259.
131. Cutting, G.R., *Cystic fibrosis genetics: from molecular understanding to clinical application*. *Nat Rev Genet*, 2015. **16**(1): p. 45-56.
132. Kamaruzaman, N.A., et al., *The Rabbit as a Model for Studying Lung Disease and Stem Cell Therapy*. *BioMed Research International*, 2013. **2013**: p. 12.
133. Fan, J. and T. Watanabe, *Transgenic rabbits as therapeutic protein bioreactors and human disease models*. *Pharmacol Ther*, 2003. **99**(3): p. 261-82.
134. Choi, H.K., W.E. Finkbeiner, and J.H. Widdicombe, *A comparative study of mammalian tracheal mucous glands*. *J Anat*, 2000. **197 Pt 3**: p. 361-72.

135. Widdicombe, J.H., *Transgenic animals may help resolve a sticky situation in cystic fibrosis*. The Journal of Clinical Investigation, 2010. **120**(9): p. 3093-3096.
136. Widdicombe, J.H., et al., *Distribution of tracheal and laryngeal mucous glands in some rodents and the rabbit*. Journal of Anatomy, 2001. **198**(Pt 2): p. 207-221.
137. Widdicombe, J.H. and J.J. Wine, *Airway Gland Structure and Function*. Physiol Rev, 2015. **95**(4): p. 1241-319.
138. Tiddens, H.A., et al., *Cystic fibrosis lung disease starts in the small airways: can we treat it more effectively?* Pediatr Pulmonol, 2010. **45**(2): p. 107-17.
139. Lukacs, G.L. and A.S. Verkman, *CFTR: folding, misfolding and correcting the DeltaF508 conformational defect*. Trends Mol Med, 2012. **18**(2): p. 81-91.
140. Amaral, M.D., *CFTR and chaperones: processing and degradation*. J Mol Neurosci, 2004. **23**(1-2): p. 41-8.
141. Cheng, S.H., et al., *Defective intracellular transport and processing of CFTR is the molecular basis of most cystic fibrosis*. Cell, 1990. **63**(4): p. 827-34.
142. Young, J.C., J.M. Barral, and F. Ulrich Hartl, *More than folding: localized functions of cytosolic chaperones*. Trends Biochem Sci, 2003. **28**(10): p. 541-7.
143. Ren, H.Y., et al., *VX-809 corrects folding defects in cystic fibrosis transmembrane conductance regulator protein through action on membrane-spanning domain 1*. Mol Biol Cell, 2013. **24**(19): p. 3016-24.
144. Van Goor, F., et al., *Rescue of DeltaF508-CFTR trafficking and gating in human cystic fibrosis airway primary cultures by small molecules*. Am J Physiol Lung Cell Mol Physiol, 2006. **290**(6): p. L1117-30.

145. Mehnert, M., T. Sommer, and E. Jarosch, *ERAD ubiquitin ligases: multifunctional tools for protein quality control and waste disposal in the endoplasmic reticulum*. *Bioessays*, 2010. **32**(10): p. 905-13.
146. Song, L. and Z.-Q. Luo, *Post-translational regulation of ubiquitin signaling*. *The Journal of Cell Biology*, 2019. **218**(6): p. 1776-1786.
147. Kumar, S., W.H. Kao, and P.M. Howley, *Physical interaction between specific E2 and Hect E3 enzymes determines functional cooperativity*. *J Biol Chem*, 1997. **272**(21): p. 13548-54.
148. Chin, L.S., J.P. Vavalle, and L. Li, *Staring, a novel E3 ubiquitin-protein ligase that targets syntaxin 1 for degradation*. *J Biol Chem*, 2002. **277**(38): p. 35071-9.
149. Moynihan, T.P., et al., *The ubiquitin-conjugating enzymes UbcH7 and UbcH8 interact with RING finger/IBR motif-containing domains of HHARI and H7-API*. *J Biol Chem*, 1999. **274**(43): p. 30963-8.
150. van Wijk, S.J., et al., *A comprehensive framework of E2-RING E3 interactions of the human ubiquitin-proteasome system*. *Mol Syst Biol*, 2009. **5**: p. 295.
151. Wang, G., et al., *Endoplasmic reticulum factor ERLIN2 regulates cytosolic lipid content in cancer cells*. *Biochem J*, 2012. **446**(3): p. 415-25.
152. Fortier, J.M. and J. Kornbluth, *NK Lytic-Associated Molecule, Involved in NK Cytotoxic Function, Is an E3 Ligase*. *The Journal of Immunology*, 2006. **176**(11): p. 6454-6463.
153. Portis, T., et al., *Gene structure of human and mouse NKLAM, a gene associated with cellular cytotoxicity*. *Immunogenetics*, 2000. **51**(7): p. 546-555.
154. Lawrence, D.W. and J. Kornbluth, *E3 ubiquitin ligase NKLAM ubiquitinates STAT1 and positively regulates STAT1-mediated transcriptional activity*. *Cell Signal*, 2016. **28**(12): p. 1833-1841.

155. Zhao, C., et al., *The UbcH8 ubiquitin E2 enzyme is also the E2 enzyme for ISG15, an IFN- $\alpha$ /beta-induced ubiquitin-like protein*. Proceedings of the National Academy of Sciences of the United States of America, 2004. **101**(20): p. 7578-7582.
156. Zhou, X., et al., *Epigenetic downregulation of the ISG15-conjugating enzyme UbcH8 impairs lipolysis and correlates with poor prognosis in nasopharyngeal carcinoma*. Oncotarget, 2015. **6**(38): p. 41077-91.
157. Ye, Y., et al., *Recruitment of the p97 ATPase and ubiquitin ligases to the site of retrotranslocation at the endoplasmic reticulum membrane*. Proc Natl Acad Sci U S A, 2005. **102**(40): p. 14132-8.
158. Yeung, H.O., et al., *Insights into adaptor binding to the AAA protein p97*. Biochem Soc Trans, 2008. **36**(Pt 1): p. 62-7.
159. Ye, Y., et al., *A Mighty "Protein Extractor" of the Cell: Structure and Function of the p97/CDC48 ATPase*. Front Mol Biosci, 2017. **4**: p. 39.
160. Stach, L. and P.S. Freemont, *The AAA+ ATPase p97, a cellular multitool*. Biochem J, 2017. **474**(17): p. 2953-2976.
161. Hou, X., et al., *Dissection of the Role of VIMP in Endoplasmic Reticulum-Associated Degradation of CFTR $\Delta$ F508*. Scientific Reports, 2018. **8**(1): p. 4764.
162. Lawrence, D.W., G. Gullickson, and J. Kornbluth, *E3 ubiquitin ligase NKLAM positively regulates macrophage inducible nitric oxide synthase expression*. Immunobiology, (0).
163. Lawrence, D.W. and J. Kornbluth, *E3 Ubiquitin ligase NKLAM is a macrophage phagosome protein and plays a role in bacterial killing*. Cellular immunology, 2012. **279**(1): p. 46-52.
164. Ceko, M.J., et al., *X-Ray fluorescence imaging and other analyses identify selenium and GPXI as important in female reproductive function*. Metallomics, 2015. **7**(1): p. 71-82.

165. Ye, L., et al., *DeltaF508-CFTR correctors: synthesis and evaluation of thiazole-tethered imidazolones, oxazoles, oxadiazoles, and thiadiazoles*. *Bioorg Med Chem Lett*, 2014. **24**(24): p. 5840-5844.
166. Le Henaff, C., et al., *Increased NF-kappaB Activity and Decreased Wnt/beta-Catenin Signaling Mediate Reduced Osteoblast Differentiation and Function in DeltaF508 Cystic Fibrosis Transmembrane Conductance Regulator (CFTR) Mice*. *J Biol Chem*, 2015. **290**(29): p. 18009-17.
167. Meng, X., et al., *Two Small Molecules Restore Stability to a Subpopulation of the Cystic Fibrosis Transmembrane Conductance Regulator with the Predominant Disease-causing Mutation*. *J Biol Chem*, 2017. **292**(9): p. 3706-3719.
168. Sturgess, J. and J. Imrie, *Quantitative evaluation of the development of tracheal submucosal glands in infants with cystic fibrosis and control infants*. *Am J Pathol*, 1982. **106**(3): p. 303-11.
169. O'Brien, S., et al., *Biliary complications of cystic fibrosis*. *Gut*, 1992. **33**(3): p. 387-91.
170. Moran, A., et al., *Protein metabolism in clinically stable adult cystic fibrosis patients with abnormal glucose tolerance*. *Diabetes*, 2001. **50**(6): p. 1336-43.
171. Park, R.W. and R.J. Grand, *Gastrointestinal manifestations of cystic fibrosis: a review*. *Gastroenterology*, 1981. **81**(6): p. 1143-61.
172. Yang, D., et al., *Effective gene targeting in rabbits using RNA-guided Cas9 nucleases*. *J Mol Cell Biol*, 2014. **6**(1): p. 97-9.
173. Song, J., et al., *Production of immunodeficient rabbits by multiplex embryo transfer and multiplex gene targeting*. *Sci Rep*, 2017. **7**(1): p. 12202.
174. Song, J., et al., *RS-1 enhances CRISPR/Cas9 and TALEN mediated knock-in efficiency*. *Nat Commun*, 2016. **7**: p. 10548. doi: 10.1038/ncomms10548.

175. Grubb, B.R., *Ion transport across the jejunum in normal and cystic fibrosis mice*. Am J Physiol, 1995. **268**(3 Pt 1): p. G505-13.
176. Grubb, B.R. and R.C. Boucher, *Pathophysiology of gene-targeted mouse models for cystic fibrosis*. Physiological reviews, 1999. **79**(1 Suppl): p. S193-214.
177. Grubb, B.R., R.N. Vick, and R.C. Boucher, *Hyperabsorption of Na<sup>+</sup> and raised Ca(2<sup>+</sup>)-mediated Cl<sup>-</sup> secretion in nasal epithelia of CF mice*. Am J Physiol, 1994. **266**(5 Pt 1): p. C1478-83.
178. Kerem, B., et al., *Identification of the cystic fibrosis gene: genetic analysis*. Science, 1989. **245**(4922): p. 1073-80.
179. Kerem, E., et al., *Clinical and genetic comparisons of patients with cystic fibrosis, with or without meconium ileus*. J Pediatr, 1989. **114**(5): p. 767-73.
180. Rosenstein, B.J. and T.S. Langbaum, *Incidence of distal intestinal obstruction syndrome in cystic fibrosis*. J Pediatr Gastroenterol Nutr, 1983. **2**(2): p. 299-301.
181. Sathe, M. and R. Houwen, *Meconium ileus in Cystic Fibrosis*. J Cyst Fibros, 2017. **16** **Suppl 2**: p. S32-s39.
182. Yan, Z., et al., *Ferret and pig models of cystic fibrosis: Prospects and promise for gene therapy*. Hum Gene Ther Clin Dev, 2015. **26**(1): p. 38-49.
183. Sun, X., et al., *Disease phenotype of a ferret CFTR-knockout model of cystic fibrosis*. J Clin Invest, 2010. **120**(9): p. 3149-60.
184. Kreda, S.M., et al., *Characterization of wild-type and deltaF508 cystic fibrosis transmembrane regulator in human respiratory epithelia*. Mol Biol Cell, 2005. **16**(5): p. 2154-67.
185. Boucher, R.C., et al., *Na<sup>+</sup> transport in cystic fibrosis respiratory epithelia. Abnormal basal rate and response to adenylate cyclase activation*. J Clin Invest, 1986. **78**(5): p. 1245-52.

186. Knowles, M.R., et al., *Abnormal ion permeation through cystic fibrosis respiratory epithelium*. Science, 1983. **221**(4615): p. 1067-70.
187. Bonvin, E., et al., *Congenital tracheal malformation in cystic fibrosis transmembrane conductance regulator-deficient mice*. J Physiol, 2008. **586**(13): p. 3231-43.
188. Meyerholz, D.K., et al., *Loss of cystic fibrosis transmembrane conductance regulator function produces abnormalities in tracheal development in neonatal pigs and young children*. Am J Respir Crit Care Med, 2010. **182**(10): p. 1251-61.
189. Meyerholz, D.K., et al., *Lack of cystic fibrosis transmembrane conductance regulator disrupts fetal airway development in pigs*. Lab Invest, 2018. **98**(6): p. 825-838.
190. Robinson, M. and P.T. Bye, *Mucociliary clearance in cystic fibrosis*. Pediatr Pulmonol, 2002. **33**(4): p. 293-306.
191. Markovetz, M.R., et al., *A physiologically-motivated compartment-based model of the effect of inhaled hypertonic saline on mucociliary clearance and liquid transport in cystic fibrosis*. PLoS One, 2014. **9**(11): p. e111972.
192. Blouquit, S., et al., *Ion and fluid transport properties of small airways in cystic fibrosis*. Am J Respir Crit Care Med, 2006. **174**(3): p. 299-305.
193. Mall, M.A., *Unplugging mucus in cystic fibrosis and chronic obstructive pulmonary disease*. Ann Am Thorac Soc, 2016. **13 Suppl 2**: p. S177-85.
194. Tiddens, H., et al., *Novel outcome measures for clinical trials in cystic fibrosis*. Pediatr Pulmonol, 2015. **50**(3): p. 302-315.
195. Khan, T.Z., et al., *Early pulmonary inflammation in infants with cystic fibrosis*. Am J Respir Crit Care Med, 1995. **151**(4): p. 1075-82.
196. Muhlebach, M.S., et al., *Quantitation of inflammatory responses to bacteria in young cystic fibrosis and control patients*. Am J Respir Crit Care Med, 1999. **160**(1): p. 186-91.

197. McMorran, B.J., et al., *Novel neutrophil-derived proteins in bronchoalveolar lavage fluid indicate an exaggerated inflammatory response in pediatric cystic fibrosis patients*. Clin Chem, 2007. **53**(10): p. 1782-91.
198. Ratjen, F., *Cystic fibrosis: the role of the small airways*. J Aerosol Med Pulm Drug Deliv, 2012. **25**(5): p. 261-4.
199. Bakker, E.M., et al., *Small airway involvement in cystic fibrosis lung disease: routine spirometry as an early and sensitive marker*. Pediatr Pulmonol, 2013. **48**(11): p. 1081-8.
200. Mellins, R.B., *The site of airway obstruction in cystic fibrosis*. Pediatrics, 1969. **44**(3): p. 315-8.
201. Zuelzer, W.W. and W.A. Newton, Jr., *The pathogenesis of fibrocystic disease of the pancreas; a study of 36 cases with special reference to the pulmonary lesions*. Pediatrics, 1949. **4**(1): p. 53-69.
202. Plopper, C.G., et al., *Distribution of nonciliated bronchiolar epithelial (Clara) cells in intra- and extrapulmonary airways of the rabbit*. Exp Lung Res, 1983. **5**(2): p. 79-98.
203. Muhlebach, M.S., et al., *Initial acquisition and succession of the cystic fibrosis lung microbiome is associated with disease progression in infants and preschool children*. PLoS Pathog, 2018. **14**(1): p. e1006798.
204. Sly, P.D., et al., *Lung disease at diagnosis in infants with cystic fibrosis detected by newborn screening*. Am J Respir Crit Care Med, 2009. **180**(2): p. 146-52.
205. Esther Jr, C.R., M.S. Muhlebach, and S.M. Stick, *Mucus in early CF lung disease*. Pediatr Pulmonol, 2018. **53**: p. 74-75.
206. Davis, S.D. and T. Ferkol, *Identifying the origins of cystic fibrosis lung disease*. N Engl J Med, 2013. **368**(21): p. 2026-8.

207. Fagerberg, L., et al., *Analysis of the human tissue-specific expression by genome-wide integration of transcriptomics and antibody-based proteomics*. Mol Cell Proteomics, 2014. **13**(2): p. 397-406.
208. Kaneko, M., et al., *Genome-wide identification and gene expression profiling of ubiquitin ligases for endoplasmic reticulum protein degradation*. Sci Rep, 2016. **6**: p. 30955.
209. Ribeiro, C.M. and R.C. Boucher, *Role of endoplasmic reticulum stress in cystic fibrosis-related airway inflammatory responses*. Proc Am Thorac Soc, 2010. **7**(6): p. 387-94.

**ABSTRACT****MOLECULAR MECHANISMS IN CFTR-F508DEL DEGRADATION AND THE FUNCTIONAL DEFECT OF CFTR ABSENCE IN RABBITS**

by

**CARTHIC RAJAGOPALAN****August 2019****Advisors:** Dr. Xuequn Chen**Major:** Physiology**Degree:** Doctor of Philosophy

Cystic Fibrosis (CF) is the most common, lethal autosomal recessive disorder, and is caused by mutations in the cystic fibrosis transmembrane conductance regulator protein (CFTR), an anion channel that is found in most epithelial cells lining the airway and gut. The most common mutation of CFTR is deletion of phenylalanine at position 508 (CFTR-F508del), which produces a misfolded protein. Through the ubiquitin proteasome system (UPS), this misfolded protein is ubiquitinated and signaled for degradation via the cytosolic proteasome. Previous studies demonstrating experimental restoration of F508DEL-CFTR trafficking to the plasma membrane showed partial function of the chloride channel, raising therapeutic speculations. Some components of how F508DEL-CFTR is degraded is known, however many mechanisms that underlie its degradation through ERAD and the UPS is still unknown. In the first part of the study we used a siRNA screen to discover the E3 ligase, RNF19B, and its interacting partner, UBE 2L6 mediates F508del degradation. We used siRNA-mediated silencing of endogenous UBE 2L6 and RNF19B in the CF human bronchial epithelial (HBE) cell line to demonstrate that there is an increase in F508del-CFTR expression. We also co-expressed UBE 2L6 and RNF 19B with F508del in HEK293 cells that demonstrated a decrease in F508del compared to control.

Cycloheximide-chase (CHX) experiments using HEK 293 cells overexpressing RNF19B and F508del showed that there was a decrease in F508del half-life. Lastly, using siRNA-mediated silencing of endogenous UBE 2L6 and RNF19B in CFBE-F508del cells increased forskolin-stimulated short-circuit currents.

Cell models have given the CF research community a tremendous amount of information about the mechanisms that underlay the disease. However, they are not suited to understand the pathophysiology of the disease. Existing animal models of CF have limitations because they either fail to exhibit key CF pulmonary phenotypes, die soon after birth, and/or require special care with high maintenance costs. In the second part of the study, we report the generation by CRISPR/Cas9 of CF rabbits, a model with a relatively long lifespan and affordable maintenance and care costs. CF rabbits untreated live for > 40 d, and therapeutic regimens directed towards restoration of intraluminal transit of gastrointestinal materials extend lifespan to > 80 days. CFTR expression in the rabbit lung mimicked expression in the human lung with widespread expression in proximal and distal lower airway epithelia. CF rabbits exhibited human-like abnormalities in airway bioelectric properties and sporadic, spontaneous polymicrobial lower respiratory tract infections in the absence of submucosal glands. The CF rabbit model may serve as a useful tool for understanding CF pathogenesis and the practical development of therapeutics for this life-shortening disease.

## AUTOBIOGRAPHICAL STATEMENT

### CARTHIC RAJAGOPALAN

**Education**      2019 Wayne State University, Detroit, MI  
                             Ph.D. Student in Physiology  
                             Advisors: Fei Sun M.D., PhD., Xuequn Chen PhD.  
                             2009 University of Waterloo, Waterloo, Ontario, Canada  
                             Bachelor of Science – Honors Kinesiology

#### Publications

1. Ruan J, Hirai H, Yang D, Ma L, Hou X, Jiang H, Wei H, **Rajagopalan C**, Mou H, Wang G, Zhang J, Li K, Chen YE, Sun F, Xu J. Efficient Gene Editing at Major CFTR Mutation Loci. *Mol Ther Nucleic Acids*. 2019 Feb 16;16:73-81. doi: 10.1016/j.omtn.2019.02.006. PMID: 30852378
2. Hou X, Wei H, **Rajagopalan C**, Jiang H, Wu Q, Zaman K, Xie Y, Sun F. Dissection of the Role of VIMP in Endoplasmic Reticulum-Associated Degradation of CFTR $\Delta$ F508. *Sci Rep*. 2018 Mar 19;8(1):4764. doi: 10.1038/s41598-018-23284-8. PMID: 29555962

#### Meetings

1. North American Cystic Fibrosis Conference, Denver, CO (2018)  
 “The E3 Ubiquitin Ligase RNF19B promotes CFTR  $\Delta$ F508 Degradation”  
 “UBE2L6 is a Ubiquitin Conjugating Enzyme that Directs CFTR  $\Delta$ F508 Degradation” 2018
2. North American Cystic Fibrosis Conference, Indianapolis, IN (2017)  
 “Absence of the CFTR Gene in Rabbits Produces Human-Like Cystic Fibrosis”  
 “Vimp-Derlin-1 Complex Recruits Ubiquitin E3 Ligase RNF5 to facilitate CFTR Degradation”
3. Michigan Physiological Society Meeting, Alma College, Alma, MI (2017)  
 “E3 Ligases and CFTR” Three-minute Thesis 2017
4. North American Cystic Fibrosis Conference, Orlando, FL (2016)  
 “VIMP Recruits Ubiquitin E3 Ligase RNF5 to the Endoplasmic Reticulum for CFTR Degradation”
5. Michigan Physiological Society Meeting, Wayne State University, Detroit, MI (2016)  
 “VIMP Recruits Ubiquitin E3 Ligase RNF5 to the Endoplasmic Reticulum for CFTR Degradation”
6. Graduate Student Research Day, Wayne State University, Detroit, MI (2015)  
 “RNF19B: A Novel E3 Ubiquitin Ligase Involved in the Proteasomal Degradation of CFTR”

#### Teaching Experience

- Wayne State University, Detroit, MI (2017-2018)  
 PSL 7020 and PSL7040-Organized and taught physiology labs in mutagenesis and transepithelial currents to physiology graduate students
- Wayne State University, Detroit, MI (2017-2019)  
 Helped coach and teach respiratory physiology to Wayne State University undergraduate students in the Michigan Physiological Quiz Bowl
- Wayne State University, Detroit, MI (2016)  
 Helped in the physiology laboratories, teaching students how to read an electrocardiogram
- Wayne State University, Detroit, MI (2016)  
 Taught graduate students how to operate and interpret data using the Ussing Chamber